ORGANOMETALLICS

Article

pubs.acs.org/Organometallics

Bulky *N*-Phosphinomethyl-Functionalized N-Heterocyclic Carbene Chelate Ligands: Synthesis, Molecular Geometry, Electronic Structure, and Their Ruthenium Alkylidene Complexes

Hiyam Salem,[†] Martin Schmitt,[‡,§] Ulrike Herrlich (née Blumbach),[‡,⊥] Erik Kühnel,[‡] Marcel Brill,[‡] Philipp Nägele,[‡] André Luiz Bogado,[‡,∥] Frank Rominger,[‡] and Peter Hofmann*[,†,‡]

[†]Catalysis Research Laboratory (CaRLa), University of Heidelberg, Im Neuenheimer Feld 584, D-69120 Heidelberg, Germany

[‡]Organisch-Chemisches Institut, University of Heidelberg, Im Neuenheimer Feld 270, D-69120 Heidelberg, Germany

Supporting Information

ABSTRACT: A new, extremely bulky, and electron-rich *N*-phosphinomethyl-functionalized N-heterocyclic carbene ligand, **5a** (^{tBu}NHCP^{tBu}), and a somewhat less bulky congener, **5b** (^{Mes}NHCP^{tBu}), forming five-membered chelate rings with metal centers, have been synthesized in four steps starting from the easily accessible di-*tert*-butyl(hydroxymethyl)phosphine oxide (**1**). **5a** was isolated and fully characterized by spectroscopic methods including UV-photoelectron spectroscopy and X-ray diffraction. The reaction of **5a** with $[Ru(COD)Cl_2]_n$ under hydrogen pressure or with $[Ru(p\text{-cymene})Cl_2]_2$ led to the formation of the unsaturated dinuclear complex $[Ru(^{tBu}NHCP^{tBu})(\mu\text{-Cl})(Cl)]_2$ (**6**), which serves as a precursor for a series of ruthenium carbene complexes (**7a–f**) using substituted phenyldiazomethanes (p-X-$C_6H_4(CH)N_2$; X = H (**a**), Br (**b**), CF_3 (**c**), NO_2, (**d**), CH_3 (**e**)) and trimethylsilyldiazomethane (**f**). Treatment of **6** with phosphine or pyridine ligands led to the formation of the mononuclear adducts, $[Ru(^{tBu}NHCP^{tBu})(Cl_2)(PR_3)]$ (R = Me (**8**), Ph (**9**), Cy (**10**)) and $[Ru(^{tBu}NHCP^{tBu})(Cl_2)(py)_n]$ (n = 1 (**11**), 2 (**12**); if $(py)_2$ = bipy (**13**)), which were synthesized in order to find alternative precursor complexes because the dimer **6** showed very low solubility in most organic solvents. Complex **7a** was obtained analytically pure on a different route via transmetalation from a silver complex bearing ^{tBu}NHCP^{tBu} (**15**) to the first-generation Grubbs catalyst as the ruthenium precursor. Complexes **7a–c** and **7e** were characterized by X-ray diffraction analysis, revealing a geometry that can be viewed as both a distorted square pyramid and a distorted trigonal bipyramid with the two chloro ligands in a *cis* configuration. The steric bulk, especially of **5a** with its *N*-*t*Bu moiety, stabilizes 16 VE Ru complexes. In contrast to ligand **5a**, the somewhat less bulky ^{Mes}NHCP^{tBu} ligand **5b** has allowed its direct metalation with two ruthenium alkylidene precursors, affording the two new carbene complexes **17** and **18**.

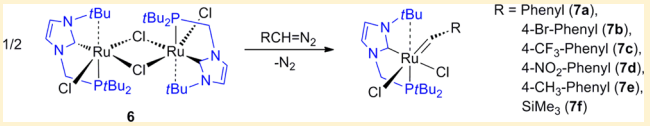

INTRODUCTION

Since the development of the first generation of Grubbs catalysts, a large variety of ruthenium alkylidene complexes for olefin metathesis have been prepared by replacing one or both of the phosphines with N-heterocyclic carbene ligands (NHCs), pyridines, chelating Schiff bases, or pyridine-alkoxides or by varying the alkylidene moiety.[1] However, the employment of chelating NHC ligands in these systems has attracted only little attention,[2] with the exception of Hoveyda's axially chiral 1,1′-binaphthyl- or 1,1′-biaryl-substituted NHC-ruthenium catalysts for asymmetric olefin metathesis[3] and the very recently introduced catalysts for *Z*-selective olefin metathesis by Grubbs et al. featuring NHC ligands with C–H-activated *N*-adamantyl groups, leading to sterically crowded five-membered chelate complexes.[4] We became interested in developing analogues of the Grubbs second-generation catalysts with sterically demanding bidentate hybrid ligands of phosphines and N-heterocyclic carbenes. Although numerous phosphino-functionalized NHC ligands have been published since the synthesis of the first representative by Herrmann et al. in 1996,[5] only two systems possess electron-rich di*alkyl*-substituted phosphino groups.[6] Moreover, the development of sterically crowded systems as the ones described within this work bearing sterically demanding groups on both the phosphorus and at one of NHC nitrogens has not yet been reported. By far, most research related to the use of NHCPs as spectator ligands in transition metal catalysis has focused on cross-coupling reactions.[5a,b,d,g,h,k,o,6a] A few papers on ruthenium coordination chemistry of NHCP ligands have been published, although neither one deals with catalysis related to olefin metathesis.[5s–v]

In previous work we have reported the synthesis of cationic ruthenium alkylidene complexes based on the bulky and electron-rich bis(di-*tert*-butylphosphino)methane (dtbpm) ligand[7] and their exceptionally high activity in ring-opening metathesis polymerization (ROMP) of, for example, cyclooctene.[8] Their neutral precursors (dtbpm)$RuCl_2$(alkylidene) resemble the square pyramidal first generation of Grubbs catalysts, but the enforced *cis* coordination of the two chloro ligands and thus their *trans* position to the phosphorus donors of the *cis*-chelating dtbpm ligand results in a facile abstraction of one of the chloro ligands even by TMS triflate. Ruthenium

Received: June 1, 2012
Published: January 2, 2013

   dx.doi.org/10.1021/om300487r | *Organometallics* 2013, 32, 29–46

Scheme 1[a]

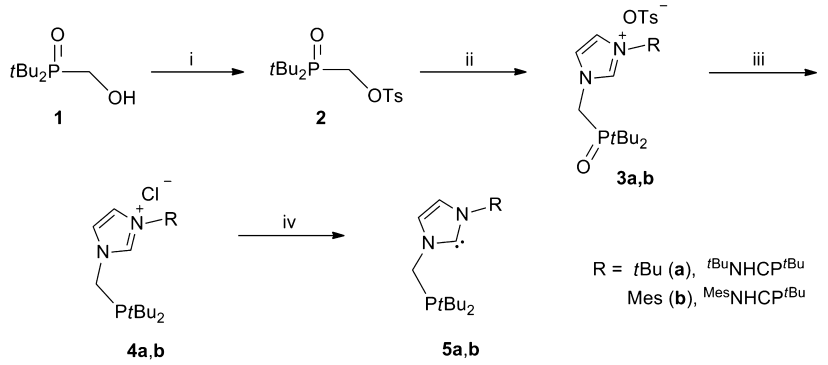

[a](i) TsCl, NEt_3, THF, 12 h, RT. (ii) **3a**: *N*-*tert*-butylimidazole, 4 d, 100 °C; **3b**: *N*-mesitylimidazole, toluene, 7 d, 120 °C. (iii) $HSiCl_3$, C_6H_5Cl, **4a**: 3 h, 120 °C; **4b**: 2 d, 80 °C. (iv) KO^{t}Bu, THF, 2 h, RT.

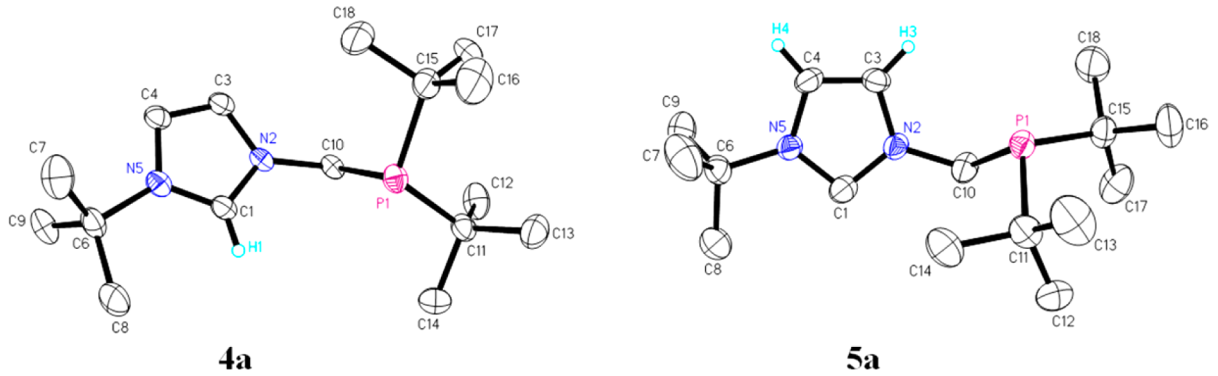

Figure 1. ORTEP plots of the cation **4a** and free NHCP **5a**. Thermal ellipsoids are at the 50% probability level. Most hydrogen atoms and the counterion are omitted for clarity. Selected bond lengths (Å) and angles (deg) of **4a**: C1−N2 = 1.332(2); C1−N5 = 1.326(3); N2−C3 = 1.384(3); N5−C4 = 1.380(3); C3−C4 = 1.353(3); N2−C1−N5 = 109.0(2); N2−C10−P1 = 111.81(14). Selected bond lengths (Å) and angles (deg) of **5a**: C1−N2 = 1.367(2); C1−N5 = 1.368(2); N2−C3 = 1.387(2); N5−C4 = 1.394(2); C3−C4 = 1.328(3); N2−C1−N5 = 101.94(15); N2−C10−P1 = 112.67(13).

alkylidene complexes of the same type with an enlarged P−Ru−P bite angle were also prepared in our group based on another bulky bisphosphine ligand, bis(di-*tert*-butylphosphino)-ethane (dtbpe),[9] and they have shown a decrease of activity in ROMP reactions compared to their analogous dtbpm-based systems.[10] In light of the high activity of the cationic ruthenium dtbpm-based complexes in ROMP reactions we have aimed at the synthesis of comparably bulky and electron-rich chelating hybrid ligands composed of an N-heterocyclic carbene moiety and an *N*-connected phosphinomethyl functionality $-CH_2-PR_2$ (called NHCP ligands in the following), appropriate for producing *cis* analogues of the second generation of Grubbs catalysts. We report herein the synthesis of such new, very bulky bidentate NHCP ligands (^{R}NHCP$^{R'}$; R = *t*Bu, Mes; R′ = *t*Bu) and their ruthenium alkylidene complexes. Complexes based on the extremely bulky system ^{tBu}NHCP^{tBu} (**5a**) were prepared by two different routes, either by utilizing diazo compounds and an electronically and coordinatively unsaturated 16 VE ruthenium dimer (**6**) based on ligand ^{tBu}NHCP^{tBu} or via transmetalation from a silver adduct of **5a** to the Grubbs first-generation catalyst. A direct metalation of the slightly less bulky ligand ^{Mes}NHCP^{tBu} (**5b**) with ruthenium alkylidene complexes as precursors is also presented. Additionally, we have studied the reactivity of dinuclear complex **6** towards phosphines and pyridines.

RESULTS AND DISCUSSION

Synthesis of Bulky *N*-Phosphinomethyl-Functionalized NHC Ligands. We have developed a convenient synthetic route to new chelating *N*-phosphinomethyl-functionalized N-heterocyclic carbene ligands (NHCPs) **5a**[11] and **5b** (Scheme 1), which were expected to form five-membered chelate rings upon metal complexation. *N*-Substituted imidazolium salts usually serve as precursors for *N*-heterocyclic carbenes and are often synthesized by nucleophilic attack of an *N*-substituted imidazole on an alkyl halide.[12] Since these reactions often require high temperatures and long reaction times, this approach initially was considered limited since substances such as R_2PCH_2X (X = leaving group) are unstable and tend to polymerize at room temperature.[13] Therefore, the corresponding phosphine oxides $tBu_2P(O)CH_2X$ were used for the synthetic route outlined in Scheme 1. They additionally allow a more convenient handling under noninert conditions.

To the best of our knowledge only three other examples of NHCP ligands with a methylene bridge between the nitrogen and the phosphorus atoms have been reported in the literature. These compounds with much less bulky diphenyl-substituted phosphine moieties were prepared from either $Ph_2P(O)CH_2Br$ or $Ph_2P(O)CH_2Cl$[5n,r] and the corresponding substituted imidazoles or by the reaction of chloromethyl-substituted benzimidazole with R_2PLi[5t,6b] (R = Ph, Cy), also leading to significantly less crowded systems than the ones described

dx.doi.org/10.1021/om300487r | *Organometallics* 2013, 32, 29−46

herein, because one of the two NHC nitrogens remains unsubstituted.

Our synthesis involves four steps starting from the known di-*tert*-butyl(hydroxymethyl)phosphine oxide **1**,[14] which was reacted with tosyl chloride in the presence of triethylamine to give the tosylate **2** in reasonable yield. Compound **2** and the N-substituted imidazole were coupled at high temperatures for several days, affording the imidazolium salts **3a,b**. In the case of *N*-*tert*-butylimidazole a temperature higher than 100 °C led to partial decomposition and a black product mixture resulting also in a decrease of the yield. When applying $t\mathrm{Bu}_2\mathrm{P(O)CH}_2\mathrm{Cl}$ instead of **2**, there was no reaction, indicating the necessity of a better leaving group. Subsequent reduction of the phosphine oxides **3a,b** using an excess of HSiCl_3 in chlorobenzene resulted in the ligand precursors **4a,b** in which the tosylate anions were completely replaced by chloride anions due to the generation of HCl during the course of the reaction.

Deprotonation of the imidazolium salts **4a,b** with K*O*t*Bu* resulted in the clean generation of the pure free carbenes **5a** and **5b**, which could be isolated as a colorless solid or a slightly yellow oil, respectively. These substances were stable under argon at −20 °C for months. Apparently, the great steric bulk created by the *t*Bu groups at the phosphorus atom together with the substituents on the imidazole moiety effectively shield the carbene carbons and thus renders the stability of these NHCP systems. The formation of the carbenes was confirmed by the absence of the H1 protons in the ^{1}H NMR and by the characteristic chemical shift of the carbene carbon signals in the $^{13}\mathrm{C}\{^1\mathrm{H}\}$ NMR spectra as singlets at 215.2 ($^{t\mathrm{Bu}}$NHCP$^{t\mathrm{Bu}}$) and 219.5 ppm ($^{\mathrm{Mes}}$NHCP$^{t\mathrm{Bu}}$). In their $^{31}\mathrm{P}\{^1\mathrm{H}\}$ NMR spectra, **5a** exhibits a singlet at 23.5 and **5b** one at 26.5 ppm. Crystals of **5a** suitable for X-ray diffraction analysis were grown by recrystallization from pentane at −20 °C (Figure 1). The bond lengths of the ring in **5a** indicate less conjugation compared to the imidazolium salt **4a**. The C−C bond in **5a** is shorter, whereas the N−C bonds are longer. The angle around C1 decreases from 109° in the imidazolium salt to 102° in the free carbene. Unfortunately, for ligand **5b** no crystal structure has been obtained so far and the crystal structure analysis of its ligand precursor **4b** was of low quality and only serves as a structural proof. The crystal structures of the imdazolium salt **4a** and free NHCP **5a** are shown in Figure 1.

UV Photoelectron Spectrum and Electronic Structure of 5a. In a UV photoelectron spectrum (He−I) the first four ionization potentials (IP) of **5a** were measured. The first ionization potential of **5a** (7.7 eV) is close to the first IP of the related electron-rich ligands bis(di-*tert*-butylphosphino)-methane (7.8 eV)[7d] and 1,3-bis-*tert*-butylimidazol-2-ylidene (7.68 eV).[15] The second to fourth ionization potentials are detected at 7.9, 8.8, and 9.4 eV, where the band at 7.9 eV is not clearly resolved and could as well be at 8.2 eV. Assuming the validity of Koopmans' theorem, which equates ionization potentials in UV-PES with the negative energies of the highest occupied molecular orbitals ($\mathrm{IP}_j = -\varepsilon_j^{(\mathrm{SCF})}$),[16] a Hartree−Fock single-point calculation (Gaussian03, HF/6-31G**)[17] using the crystal structure geometry of **5a** was performed to help assign the ionization potentials to the particular molecular orbitals. The results are listed in Table 1.

The differences Δ_j between the experimental ionization energies IP_j and the orbital energies $-\varepsilon_j$ are around 0.4 eV, which, like for a series of previously published diphosphino-methanes,[7d] can be referred to an electronic relaxation after the ionization process. The large and very electron-rich *tert*-butyl groups can act as potential electron reservoirs and are able to efficiently delocalize the positive charge resulting from the valence shell ionizations. A geometric relaxation after the ionization process is less likely to happen, as it will be much slower than the ionization process in the photoelectron experiment. Therefore, the orbital energies can be correlated to the ionization energies by shifting the values by the differences between the HOMO energies and the first ionization potentials; $\Delta_1 = -\varepsilon_{1(\mathrm{SCF})} - \mathrm{IP}_1 \approx 0.4$ eV. Thus, the photoelectron spectrum is reproduced well, and the ligand HOMO is attributed to a molecular orbital that is the antibonding combination of the π_3 orbital of the NHC ring with the phosphorus lone pair $\pi_{3\mathrm{NHC}}-\mathrm{lp}_\mathrm{P}$ (with the larger contribution of the NHC π-system to this MO, Figure 2). The HOMO−1 displays more P-lone-pair character, and the HOMO−2 is represented mainly by the carbene carbon lone pair in the NHC plane. We note that within the frame of assigning the MO character as shown, the P-arm of NHCP **5a** may well be a somewhat stronger σ-donor center than the NHC carbon in this system.

Table 1. Ionization Potentials (IP_j) of $^{t\mathrm{Bu}}$NHCP$^{t\mathrm{Bu}}$ (5a) from the UV Photoelectron Spectrum Compared to the Computed (HF/6-31G) Orbital Energies ($-\varepsilon_j$)**

PES	HF calculation			
IP_j	$-\varepsilon_j$	$-\varepsilon_j - \Delta_1$	assignment	
7.7	8.12	7.7	(NHC-π3) − (P-σ(lp))	HOMO
(7.9/8.2)	8.61	8.2	(NHC-π3) + (P-σ(lp))	HOMO−1
8.8	9.15	8.7	(NHC-σ(lp))	HOMO−2
9.4	9.84	9.4	(NHC-π2)	HOMO−3

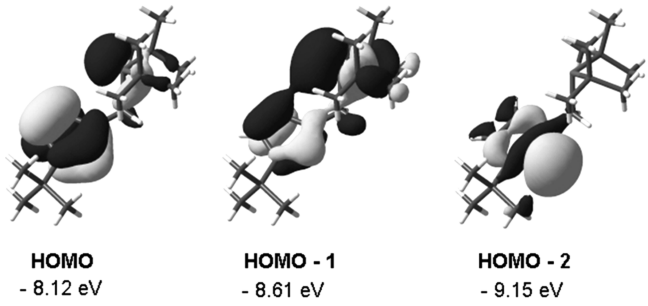

Figure 2. Calculated (HF/6-31G**) HOMOs and orbital energies of **5a** (eV).

Synthesis of 16 VE Ruthenium(II) Dimer 6 Based on NHCP 5a. A dinuclear ruthenium complex based on ligand **5a** was synthesized via two different routes. Similarly to a procedure we reported earlier on the synthesis for the dinuclear 16 VE dihydride $[(\mathrm{dtbpm})\mathrm{Ru(H)}(\mu\text{-Cl})]_2$,[18] our first route involves the reaction of the precursor $[\mathrm{Ru(COD)Cl}_2]_n$ (COD = 1,5-cyclooctadiene) with **5a** under hydrogen pressure in THF at 80 °C, affording complex **6** in 79% yield (Scheme 2). Unlike in the analogous reaction using the bisphosphine dtbpm, no hydrido complex was obtained; thus no base (e.g., triethylamine) was needed for the synthesis of **6**. Complex **6** is obtained both in the presence and absence of base. Moreover, although **6** contains no hydrides or dihydrogen ligands, the presence of H_2 was necessary, presumably for hydrogenating off the cyclooctadiene ligands. Indeed cyclooctane can be identified in the reaction solution by NMR and GC. Most probably, COD can interfere somehow with the formation of **6**, as evidenced by

dx.doi.org/10.1021/om300487r | *Organometallics* 2013, 32, 29−46

Scheme 2[a]

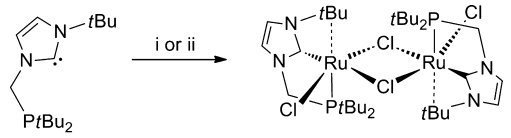

5a 6

[a](i) $[RuCl_2(COD)]_n$, H_2 (18 bar), THF, 80 °C, 3 d (79%). (ii) $[Ru(p\text{-cymene})Cl]_2$, toluene, 80 °C, 18 h (68%).

the reaction of $[Ru(COD)Cl_2]_n$ carried out in the absence of H_2, leading to substantial formation of unidentified byproducts. In a second, more convenient route, the dinuclear $[Ru(p\text{-cymene})Cl_2]_2$ precursor was reacted with **5a** in benzene at 80 °C, resulting in **6** with a slightly lower yield of 68% (Scheme 2).

Crystals of **6** suitable for X-ray diffraction analysis were obtained by slow evaporation of its solution in dichloromethane. The crystal structure of **6** revealed molecules of C_i symmetry with two unsaturated 16 VE ruthenium(II) centers, where each ruthenium is in a square pyramidal coordination geometry with the phosphines *trans* to the two empty coordination sites in apical positions (Figure 2). Moreover, the structure suggests an interaction between one of the C−H bonds of the *N*-*t*Bu groups and the ruthenium centers (indicated by the dotted lines in Scheme 2 and Figure 3).

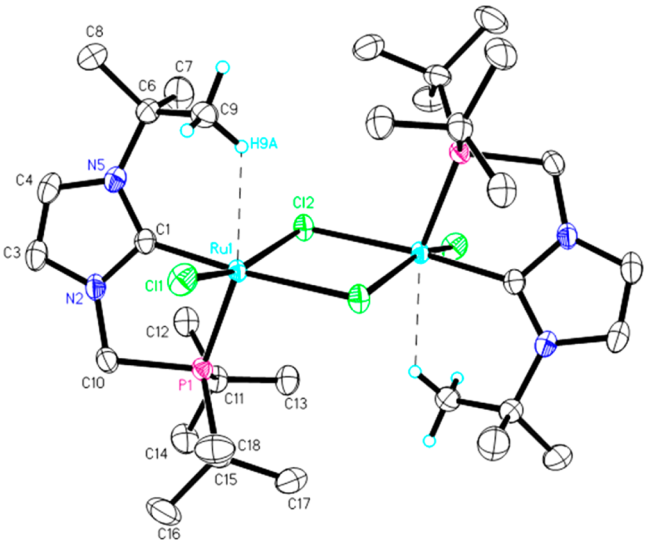

Figure 3. ORTEP plot of **6**. Thermal ellipsoids are at the 50% probability level. Most hydrogen atoms are omitted for clarity. Selected bond lengths (Å) and angles (deg): Ru1−C1 = 1.9757(18); Ru1−P1 = 2.2153(5); Ru1−Cl1 = 2.3763(5); Ru1−Cl2 = 2.4382(4); Ru1−Cl2#1 = 2.5201(4); Ru1−Ru1#1 = 3.761; C1−Ru1−P1 = 82.20(5); C1−Ru1−Cl1 = 85.16(5); C1−Ru1−Cl2 = 100.27(5); C1−Ru1−Cl2#1 = 173.47(5); P1−Ru1−Cl1 = 98.523(18); P1−Ru1−Cl2 = 102.599(16); P1−Ru1−Cl2#1 = 103.692(17); Cl1−Ru1−Cl2 = 158.705(17); Cl1−Ru1−Cl2#1 = 91.130(16); Cl2−Ru1−Cl2#1 = 81.337(15); Ru1−Cl2−Ru1#1 = 98.663(15).

The Ru−H9A and Ru−C9 distances are 2.39 and 3.07 Å, respectively, and the H9A−Ru-C9 angle is 126°. Given the fact that the Ru centers in **6** are coordinatively unsaturated and thus electron deficient, and taking into account that the Ru atoms are in a five-coordinate environment, which is the remnant of an octahedron with one ligand missing (*trans* to the phosphorus), the CH_3/Ru interaction could be tentatively interpreted as an agostic bonding situation, involving a three-center−two-electron M−H−C interaction.[19,20] Yet, indications of a strong agostic Ru−H−C bonding were not observed for **6**. The chemical shifts of all (NMR-equivalent) methyl units of the *N*-*t*Bu groups are in the range of uncoordinated C−H bonds as reported in the literature. Unlike in a similar dinuclear, cationic bisphosphine Ru complex reported by us some time ago,[8] where a substantially strong agostic interaction of the two 16 VE Ru centers with only one methyl group of two P-bound *t*Bu units was obvious from spectroscopic data and leads to a frozen orientation of the *t*Bu groups (even in solution) with rotating agostic methyl units, free rotation of the N-*t*Bu substituents is observed for **6**, even at low temperatures. It therefore seems reasonable to view the relative stability of the 16 VE complex **6** as caused by the steric shielding of both empty coordination sites of the ruthenium centers by weakly interacting *t*Bu groups, simply as a geometric consequence of the NHCP-ruthenium chelate structure, which forces these hydrocarbon fragments into their observed position. If one optimizes the geometry of **6** by DFT [Turbomole 5.7, (BP86/SV(P)] starting from the X-ray geometry, the final minimum energy structure reproduces the structure in the crystal very well, with a Ru−H9A distance of 2.37 Å and with all C−H bonds of the N-*t*Bu groups having indistinguishable lengths.

The bridging Ru−Cl bond lengths of **6** are 2.4382(4) and 2.5201(4) Å, with the Ru−Cl distance *trans* to the NHC distinctly longer due to the stronger *trans* influence of the better σ-donor NHC compared to the terminal chloride *trans* to the other μ-Cl. As expected, the terminal Ru−Cl bond is slightly shorter (2.3763(5) Å) than both bridging Ru−Cl bonds.

In its $^{31}P\{^1H\}$ NMR spectrum, complex **6** exhibits two singlets at 133.5 and 131.7 ppm in a ratio of approximately 1.4:1. Two sets of signals are also observed in the ^1H and $^{13}C\{^1H\}$ NMR spectra. This suggests the presence of at least two diastereomers in solution, from which the achiral species **6** crystallizes preferentially. Variable-temperature $^{31}P\{^1H\}$ NMR experiments (293−198 K) show a reversible variation in the ratio of the two signals, reaching approximately the inverse ratio of the room-temperature spectrum at the lowest accessible temperature (198 K), suggesting a dynamic structural process for the interconversion of diastereomers. If one considers how many diastereomers of **6** are conceivable in principle (under the sterically reasonable assumption of an apical P-coordination *trans* to the *t*Bu-shielded empty coordination site as in **6** above), then one can discuss the following structures **6a**−**c** (Scheme 3; other stereoisomers according to molecular models suffer from severe steric repulsions).

6a has C_2-symmetry and is racemic (C_2 axis through the two μ-Cl atoms), achiral **6b** has C_s-symmetry, and **6c** again is a chiral structure of C_2-symmetry (C_2 axis perpendicular to the $(\mu\text{-Cl})_2Ru_2$ plane), formed as a racemic mixture. In order to qualitatively assess the relative energies of all diastereomers of **6**, we have performed DFT calculations (Turbomole 5.7, [BP86/SV(P)])[21] for **6** and **6a**−**c**. Geometry optimization resulted only in energy minima for **6** and **6a**; the latter is found to be less stable than the isolated **6** by 36 kJ/mol (gas phase) and 38 kJ/mol (CH_2Cl_2 as solvent, modeled through COSMO[22]). The structural alternatives **6b** and **6c** do not converge to local energy minima because in both diastereomers apparently prohibitive steric repulsions between the *t*Bu groups of the phosphorus functionalities are present. The finding by DFT of only **6** and **6a** as reasonable structural proposals for

dx.doi.org/10.1021/om300487r | *Organometallics* 2013, 32, 29−46

Scheme 3

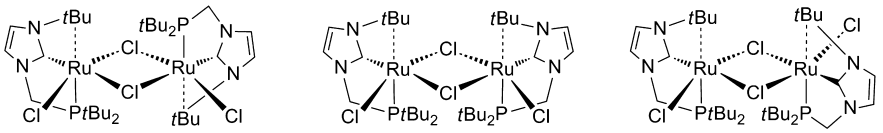

6a (C_2, rac) **6b** (C_s) **6c** (C_2, rac)

Scheme 4

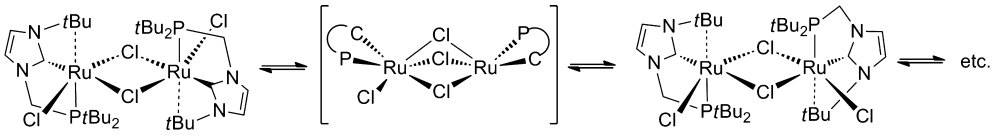

6 **6a**

Scheme 5

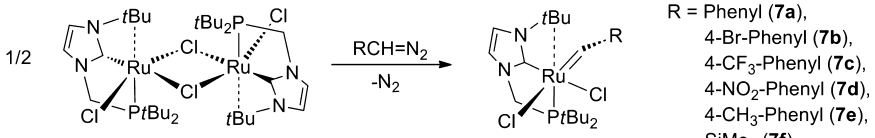

6

species in solution, with **6** being more stable, is consistent with our experimental results.

The mutual interconversion of **6** and **6a** in solution could occur through different mechanistic pathways. One possibility is the intermediacy of triply chloro-bridged ruthenium dimers (as intermediate or transition state), as displayed schematically in Scheme 4. Similar structures have been suggested by James and co-workers. These authors have prepared triply chloro-bridged ruthenium dimers based on chelating bisphosphine ligands,[23] which supports the potential existence of the triply chloro-bridged intermediate of Scheme 4 in our system. Unfortunately, when we attempted to redissolve crystals of samples, for which the solid-state structure of **6** had been elucidated by X-ray diffraction, their extremely low solubility in organic solvents prevented us from drawing firm conclusions about the postulated other isomer.

New Ruthenium(II) Alkylidene Complexes Based on ^{tBu}NHCP^{tBu} (5a). Similarly to the synthesis of first-generation Grubbs catalysts, which are accessible by the addition of phenyl diazomethane to $RuCl_2(PPh_3)_3$ followed by ligand exchange of PPh_3 with PCy_3,[24] we treated compound **6** with several phenyldiazomethanes (*p*-X-$C_6H_4(CH)N_2$; X = H (**a**), Br (**b**), CF_3 (**c**), NO_2 (**d**), CH_3 (**e**)), leading to the formation of the corresponding alkylidene complexes **7a**–**e** (Scheme 5). In the case of phenyldiazomethane we were able to isolate the ruthenium-NHCP complex (**7a**, Scheme 5). Using a different route (*vide infra*) to prepare **7a**, this Ru-carbene could be fully characterized including elemental analysis and X-ray structure. Although **7a**–**e** when made on the phenyldiazomethane route were contaminated with impurities, we were also able to obtain suitable crystals for X-ray diffraction analysis for **7b**,**c**,**e**, revealing in all cases a geometry in between a square pyramid and a trigonal bipyramid. Slow addition of solutions of the phenyldiazomethanes to suspensions of **6** in dichloromethane at 0 °C generally led to the best results. Due to the low solubility and slow reaction of the dimer **6**, the main contaminants in these reactions were the corresponding *E*/*Z* olefins formed from the phenyldiazomethanes used, which could not be fully removed without product loss.[25]

Complexes **7a**–**e** exhibit singlet signals in the range 130.7–133.0 ppm in their $^{31}P\{^1H\}$ NMR spectra. The alkylidene protons in the ^1H NMR spectra appear as doublets at 14.97–15.10 ppm with coupling constants between 8.4 and 8.8 Hz. The signals for the alkylidene carbons are found at the expected characteristic chemical shifts as doublets or broad singlets at 291.6–295.6 ppm in the $^{13}C\{^1H\}$ NMR spectra.

A ruthenium alkylidene complex (**7f**) bearing a trimethylsilyl-substituted alkylidene moiety was obtained by the utilization of the commercially available trimethylsilyl diazomethane. In contrast to the usage of the phenyldiazomethanes the reaction had to be carried out at 60 °C (Scheme 5). The proton and carbon signals of the alkylidene moiety in complex **7f** are shifted downfield compared to complexes **7a**–**e**; the alkylidene proton appears at 18.93 ppm in the ^1H NMR spectrum as a doublet ($^3J_{H,P}$ = 3.4 Hz), and the alkylidene carbon appears as a broad singlet at 354.9 ppm in the $^{13}C\{^1H\}$ NMR spectrum. In the $^{31}P\{^1H\}$ NMR spectrum complex **7f** exhibits a singlet at 124.6 ppm, which is slightly upfield compared to complexes **7a**–**e**. Crystals of **7f** suitable for X-ray analysis were obtained by slow evaporation of its CH_2Cl_2 solution. The crystal structure revealed, as for the previous cases, a distorted square pyramidal geometry (see below, Figure 4).

For the ruthenium alkylidene complex **7c** with the *p*-CF_3 substituent the quality of the crystal structure (R1 = 0.1479) only allows to safely confirm the overall structure as shown in the Supporting Information, without enabling us to discuss geometric details. In all systems, however, if considered as square pyramids and octahedral fragments, the phosphorus atom of the NHCP ligand is in the apical position and *trans* to the empty coordination site. Similarly to the (dtbpm)-$RuCl_2$(alkylidene) systems previously reported by us,[18] the two chloro ligands are situated *cis* to each other; however for **7a**–**e** the alkylidene fragment is not the apex of a square pyramid as in the bisphosphine systems but is located *trans* to one of the chlorides. Actually, a description of the molecular

dx.doi.org/10.1021/om300487r | *Organometallics* 2013, 32, 29–46

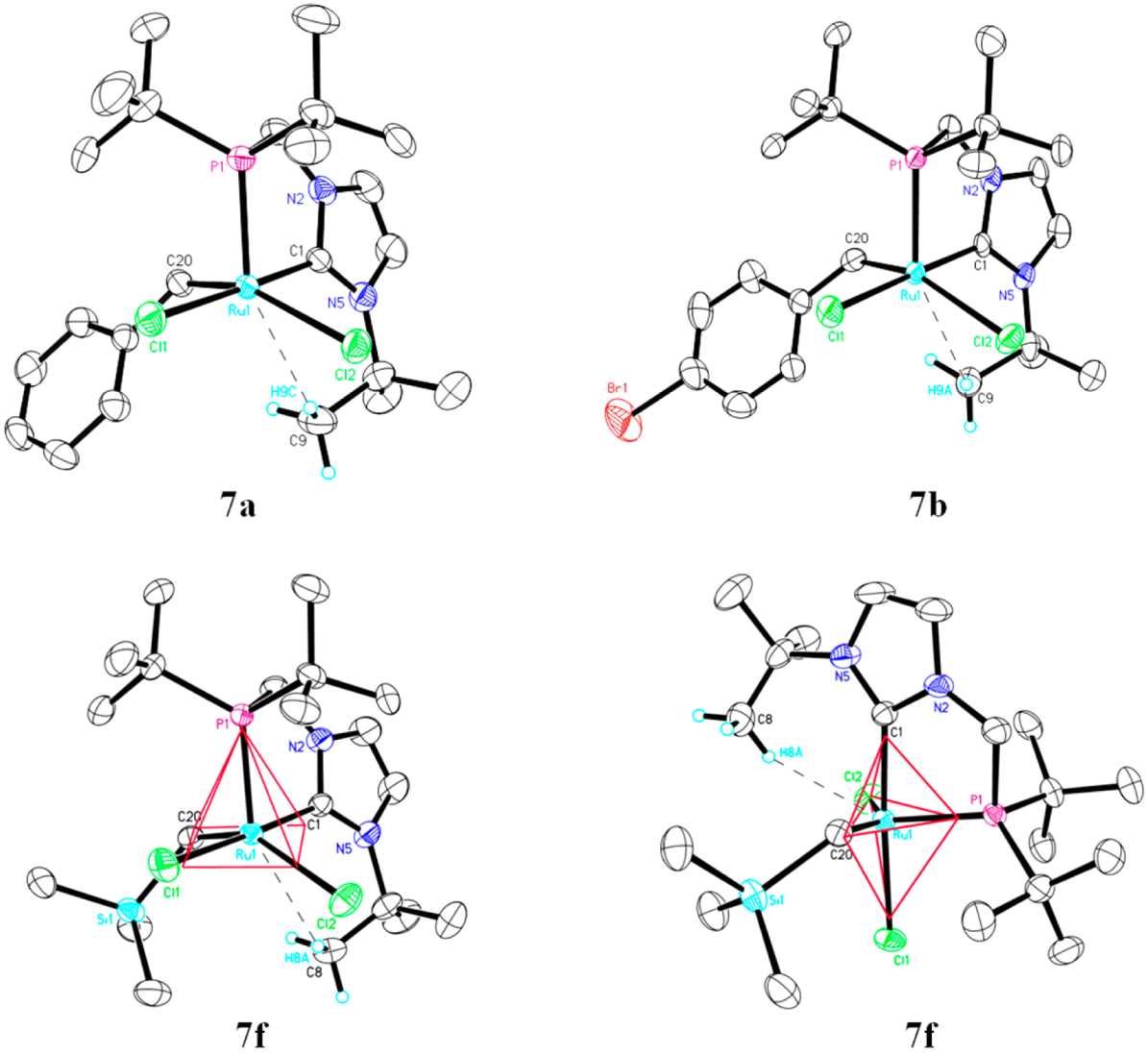

Figure 4. ORTEP plots of **7a**,**b**,**f**. Thermal ellipsoids are at the 50% probability level. Hydrogen atoms are omitted for clarity. For **7f** two orientations are shown, exemplifying the two equally possible descriptions as square pyramid or as trigonal bipyramid. Structures of **7c**,**e** are given in the Supporting Information.

Table 2. Selected Bond Lengths (Å) and Angles (deg) of 7a−c,e,f[a]

	7a	7b	7c	7e	7f
Ru1−C1	2.035(3)	2.046(7)	2.031(16)	2.045(2)	2.080(2)
Ru1−Cl1	2.4339(8)	2.4047(17)	2.389(4)	2.4182(7)	2.4203(6)
Ru1−Cl2	2.4864(8)	2.4987(19)	2.452(5)	2.5024(7)	2.4704(7)
Ru1−P1	2.2175(8)	2.2369(19)	2.212(5)	2.2236(7)	2.2354(6)
Ru1−C20	1.883(3)	1.887(8)	1.833(17)	1.880(3)	1.849(3)
C1−Ru1−Cl1	178.70(9)	178.57(19)	175.6(5)	177.79(7)	176.53(7)
C1−Ru1−Cl2	92.35(8)	111.34(7)	112.61(17)	112.51(3)	118.39(3)
Cl1−Ru1−Cl2	87.89(3)	86.36(6)	86.69(17)	86.33(3)	85.61(2)

[a]For **7c** see text.

geometries as distorted trigonal bipyramids, with one Cl and the NHC carbon being in the axial positions and the equatorial positions being coordinated by the other Cl, the alkylidene, and the phosphorus atom, is equally reasonable (as expected from the location of both structure types on pseudorotation itineraries of such d^6-ML_5 species). In this context we note that the C1−Ru−Cl1 angles are all very close to 180°, in agreement with our description (see Table 2). Starting from eight different idealized coordination geometries of compound **7f**, both square pyramidal and trigonal bipyramidal, we have performed geometry optimizations by DFT calculations [Turbomole 5.7, BP86/SV(P)]. The global minimum is practically identical to the geometries found by X-ray crystallography. Like dimer **6**, complexes **7a**,**b**,**c**,**e**,**f** also show an interaction of one of the methyl groups of the *N*-*t*Bu group with the metal center. The corresponding bond distances are

dx.doi.org/10.1021/om300487r | *Organometallics* 2013, 32, 29−46

longer compared to those observed in complex **6** and are listed in Table 3. In all structures **7a,b,c,e,f**, the Ru−Cl bonds *trans* to the NHC carbon are consistently shorter than those *trans* to the alkylidene carbon.

Table 3. Distances and Angles for the Closest CH_3/Ru Contacts of Complexes 7a,b,c,e,f

	7a	7b	7c	7e	7f
Ru1−H (Å)	2.57	2.67	2.63	2.57	2.57
Ru1−C (Å)	3.27	3.24	3.28	3.21	3.27
Ru1−H−C (deg)	128	117	123	123	128

Reactions of Complex 6 with Phosphines and Pyridines. In view of the above-mentioned low solubility of compound **6** and thus its sluggish reactivity, we have aimed at breaking the dimeric structure and transforming it into mononuclear complexes that might serve better for the synthesis of NHCP ruthenium alkylidene complexes. For this we have treated complex **6** with pyridine and also tested its reactivity toward phosphines. Complex **6** does react with phosphines PR_3 (R = Me, Ph, Cy), resulting in the formation of mononuclear complexes. In the case of PMe_3, the clean formation of complex **8** was observed (Scheme 6). It exhibits two doublets at −3.5 ($^2J_{P,P}$ = 19.2 Hz) and 122.2 ppm ($^2J_{P,P}$ = 19.2 Hz) in its $^{31}P\{^1H\}$ NMR spectrum for the two different phosphorus atoms. The protons of the bridging methylene and of the *t*Bu groups on the phosphine are not split by additional coupling with a second phosphine, even at low temperatures (−60 °C). At those temperatures the system must still be so dynamic that on average it displays C_s symmetry with an on average planar chelate ring. The solid-state structure of **8** was confirmed by X-ray diffraction analysis, revealing a geometry described best as a distorted square pyramid, where the phosphine of the NHCP ligand is again *trans* to the empty coordination site. The two chloro ligands, however, are *trans* to each other (angle Cl−Ru−Cl = 155.3°), resulting in a less sterically hindered configuration. In the $^{31}P\{^1H\}$ NMR spectrum of analytically pure complex **8** another minor set of signals was observed (in approximately a 1:50 ratio to **8**) as doublets at −5.5 and at 120.7 ppm ($^2J_{P,P}$ = 19.2 Hz), which most likely belongs to the *cis* isomer, which could not be isolated.

When treating complex **6** with PPh_3 instead of PMe_3, two sets of doublets are observed in the $^{31}P\{^1H\}$ NMR spectrum in a 5:3 ratio at 34.1 and 126.0 ppm ($^2J_{P,P}$ = 32.3 Hz) and at 24.5 and 108.3 ppm ($^2J_{P,P}$ = 10.0 Hz). Crystals obtained from this reaction have revealed a different square planar isomer than in the case of PMe_3 **8** in the solid state. The PPh_3 in complex **9b** is coordinated *trans* to one of the chlorides, which are positioned *cis* to each other (Scheme 6, Figure 5). The overall geometry of **9b** is similar to all previous complexes. The isolated complex **9b** can be the dominant isomer over **9a**; however, this crystal might also not be representative, if **9b** just crystallizes preferentially. Pyridine-functionalized phosphine ruthenium(II) complexes resembling our systems were reported by Lavigne and co-workers.[26] They have observed two isomers as well, the *cis* and *trans* dichlorides. In their case, the *cis* isomer is the thermodynamic product, which would be consistent with our result of obtaining crystals of **9b** and not **9a**.

Similarly, the addition of PCy_3 to complex **6** has led to the formation of two new sets of signals, in a 1:1 ratio, which appear as singlets instead of displaying the expected doublets (**10a,b**, Scheme 6). This reaction was less clean, and further characterization could not be achieved. So in the case of the much more bulky PCy_3 we cannot safely assign the solution or solid-state structure and tentatively assume **10a** and **10b**.

The Ru−H8 and Ru1−C8 distances (for the numbering see Figure 5) are 2.61 and 3.14 Å for **8** and 2.84 and 3.50 Å for **9b**, respectively. The Ru1−H−C8 angle is 114° for **8** and 126° for **9b**. Compared to the case of complex **6**, the CH_3/Ru interaction for **8** and **9b** is even weaker. For compound **9b** one might have expected that the Ru−Cl bond *trans* to the NHC should be lengthened compared to the one *trans* to the PPh_3 ligand, but within experimental error they are indiscernible.

Other mononuclear complexes starting from compound **6** could be synthesized by the addition of pyridine ligands. Upon dissolving complex **6** in pyridine, the dimer breaks up to give an octahedral complex (**11**, Scheme 7) with two coordinated pyridine molecules, as revealed by the crystal structure (Figure 6). Crystals suitable for X-ray analysis were obtained by concentration of a solution of **11** in pyridine followed by slow evaporation. The chlorides are positioned *trans* to each other, and the pyridines are positioned *cis* to each other, where one pyridine is *trans* to the NHCP phosphine and the other *trans* to the NHC carbon. The Ru1−N21 and Ru1−N31 bond lengths are 2.169(4) and 2.186(4) Å, respectively. In contrast to what one might have expected, but not contradicting our conclusions from the UV-PES of **5a**, the Ru1−N21 bond that is *trans* to the σ-donor NHC ligand is slightly shorter than the Ru1−N31 bond that is *trans* to the phosphine unit $PtBu_2$. In this context,

Scheme 6

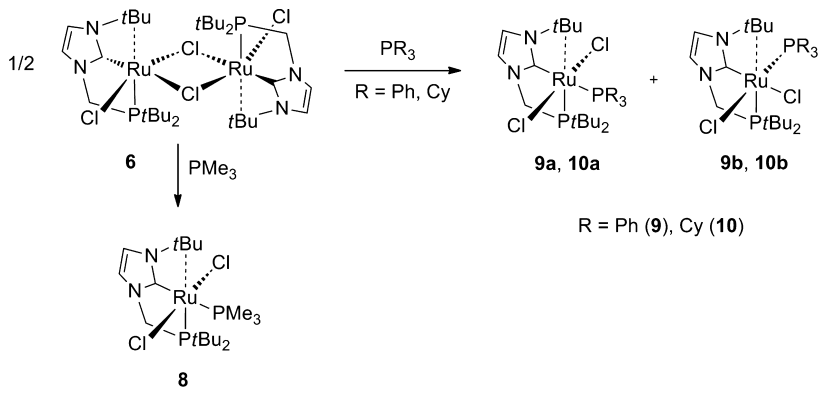

dx.doi.org/10.1021/om300487r | Organometallics 2013, 32, 29−46

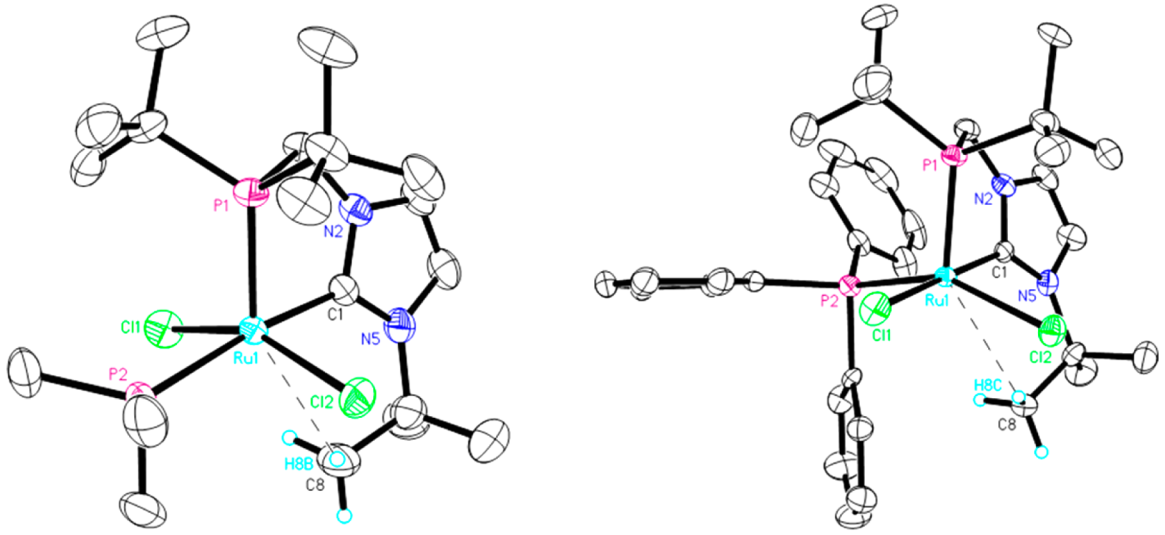

8 9b

Figure 5. ORTEP plots of **8** and **9b**. Thermal ellipsoids are at the 50% probability level. Hydrogen atoms are omitted for clarity, except for the methyl groups of the *N*-*t*Bu group blocking the empty coordination site of the ruthenium atom. Selected bond lengths (Å) and angles (deg) of **8**: Ru1−C1 = 2.049(2); Ru1−P1 = 2.2153(7); Ru1−P2 = 2.3586(7); Ru1−Cl1 = 2.3990(7); Ru1−Cl2 = 2.4239(7); C1−Ru1−P1 = 82.12(7); P2−Ru1−Cl1 = 88.50(3); C1−Ru1−P2 = 172.13(7); C1−Ru1−Cl2 = 93.21(7); P1−Ru1−P2 = 105.67(3); P1−Ru1−Cl2 = 103.52(3); C1−Ru1−Cl1 = 88.83(7); P2−Ru1−Cl2 = 86.15(3); P1−Ru1−Cl1 = 101.16(3); Cl1−Ru1−Cl2 = 155.28(3). Selected bond lengths (Å) and angles (deg) of **9b**: Ru1−P2 = 2.3164(14); Ru1−Cl1 = 2.4416(15); Ru1−Cl2 = 2.4364(14); Ru1−C1 = 2.036(5); Ru1−P1 = 2.2380(15); C1−Ru1−P1 = 80.95(15); P2−Ru1−Cl2 = 152.09(5); C1−Ru1−P2 = 89.14(15); C1−Ru1−Cl1 = 175.99(15); P1−Ru1−P2 = 102.71(5); P1−Ru1−Cl1 = 97.85(5); C1−Ru1−Cl2 = 93.00(15); P2−Ru1−Cl1 = 94.87(5); P1−Ru1−Cl2 = 105.10(5); Cl1−Ru1−Cl2 = 83.60(5).

Scheme 7

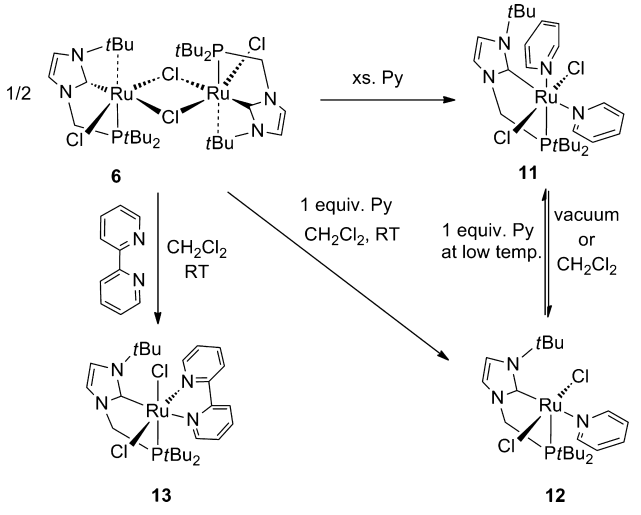

we note here that Fürstner et al. have structurally characterized a Grubbs II type ruthenium benzylidene complex with two *cis*-ligated chloro ligands and with one NHC and one PCy_3 ligand, both also *cis* to each other.[2a] In this compound the Ru−Cl bond *trans* to the NHC unit is also shorter than Ru−Cl *trans* to PCy_3. Furthermore, we note parenthetically that as with phosphines and pyridines the Ru dimer **6** also reacts with CO to yield an octahedral *trans*-dichloro complex $[RuCl_2(^{t\mathrm{Bu}}\mathrm{NHCP}^{t\mathrm{Bu}})(CO)_2]$ with a CO ligand *trans* to the NHC-carbon and the other *trans* to the $t\mathrm{Bu}_2\mathrm{P}$ unit, respectively. Its X-ray structure (given in the Supporting Information, compound **A**) also points to the P-arm of **5a** to have the stronger *trans* influence.

A mononuclear complex that bears only one pyridine molecule was obtained by addition of one equivalent of pyridine per ruthenium center of complex **6**. The resulting complex **12** could also be obtained by long-term drying of **11** under vacuum or by addition of CH_2Cl_2 to **11**. We have also observed a conversion of **11** to **12** in low-temperature NMR experiments. Crystals of **12** could not be obtained. The geometry is most likely similar to that of the mononuclear complexes **8** and **9b**, as evidenced from the NMR data. The presence of only one pyridine molecule is further confirmed by mass spectroscopy.

Disappointingly, treatment of the monopyridine complex **12** with phenyldiazomethanes did not result in the desired alkylidene complexes. The pyridine molecule is apparently too strongly bound to the metal center; its replacement with an alkylidene fragment does not take place. To address this problem, substituted pyridines such as 2,6-dibromo- and 2,6-dimethylpyridine were also applied, hoping for a weaker coordination of only one pyridine molecule per ruthenium center induced by their increased steric bulk. Upon treatment of complex **6** with these substituted pyridines, we have obtained only mixtures of undefined products.

The bidentate ligand 2,2′-bipyridine reacts with **6**, resulting in the formation of complex **13**, the structure of which was confirmed by X-ray analysis (Figure 6). The crystal structure revealed a distorted octahedral geometry where the two chlorides are positioned *cis* to each other and *trans* to one of the pyridine rings and the phosphine. According to NMR data, only this isomer is present in solution. In the $^{31}P\{^1H\}$ NMR spectrum complex **13** exhibits one singlet at 119.4 ppm and in the ^1H NMR spectrum two different sets of signals for the bipyridine protons are present, supporting the nonequivalence of the two rings. An isomer of **13** where the two chlorides are

dx.doi.org/10.1021/om300487r | *Organometallics* 2013, 32, 29−46

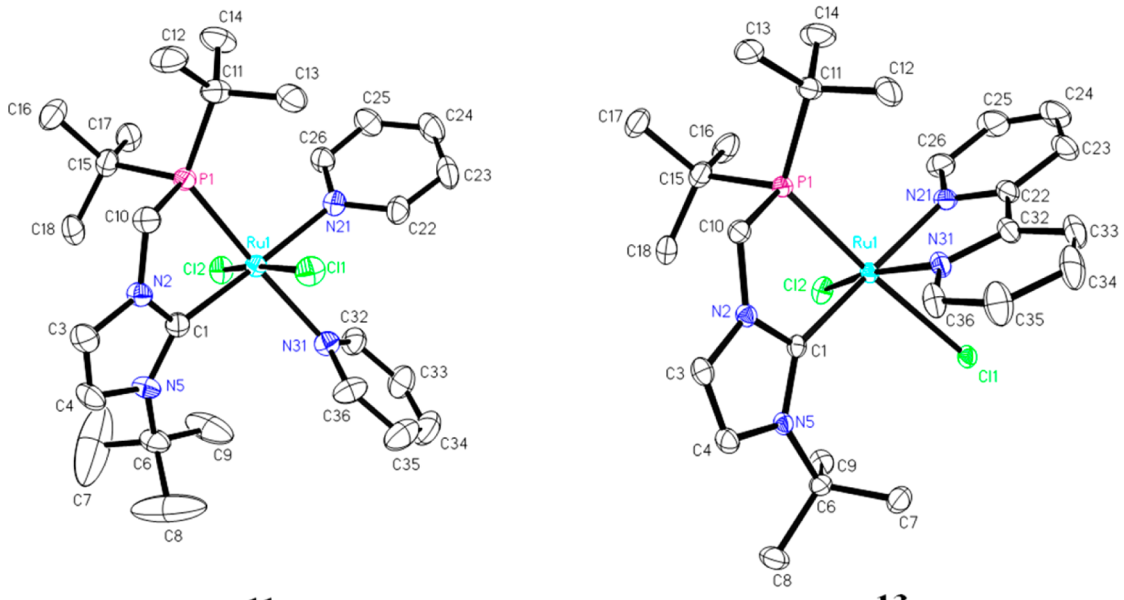

Figure 6. ORTEP plots of **11** and **13**. Thermal ellipsoids are at the 50% probability level. Hydrogen atoms are omitted for clarity. Selected bond lengths (Å) and angles (deg) of **11**: Ru1−P1 = 2.3139(11); Ru1−C1 = 2.086(4); Ru1−N21 = 2.169(4); Ru1−N31 = 2.186(4); Ru1−Cl1 = 2.4488(10); Ru1−Cl2 = 2.4319(10); C1−Ru1−N31 = 99.90(15); N31−Ru1−Cl2 = 88.47(9); N21−Ru1−N31 = 82.56(13); P1−Ru1−Cl2 = 97.36(4); C1−Ru1−P1 = 80.85(12); C1−Ru1−Cl1 = 85.73(11); N21−Ru1−P1 = 96.29(10); N21−Ru1−Cl1 = 90.65(9); N31−Ru1−P1 = 173.99(9); N31−Ru1−Cl1 = 83.91(9); C1−Ru1−Cl2 = 97.21(11); P1−Ru1−Cl1 = 90.21(4); C1−Ru1−N21 = 175.37(14); N21−Ru1−Cl2 = 86.75(9); Cl2−Ru1−Cl1 = 172.21(4). Selected bond lengths (Å) and angles (deg) of **13**: Ru1−P1 = 2.2962(6); Ru1−C1 = 2.094(2); Ru1−Cl1 = 2.5217(5); Ru1−Cl2 = 2.4292(6); Ru1−N21 = 2.0924(18); Ru1−N31 = 2.0372(19); N31−Ru1−N21 = 79.10(8); N31−Ru1−C1 = 91.59(7); N21−Ru1−C1 = 170.34(8); N31−Ru1−P1 = 96.85(5); N21−Ru1−P1, 97.03(5); N31−Ru1−Cl2 = 164.54(5); N21−Ru1−Cl2 = 92.15(6); C1−Ru1−Cl2 = 97.50(6); C1−Ru1−P1 = 81.40(6); P1−Ru1−Cl2 = 96.85(2); N31−Ru1−Cl1 = 81.27(5); N21−Ru1−Cl1 = 79.25(5); C1−Ru1−Cl1 = 102.06(6); P1−Ru1−Cl1 = 176.072(19); Cl2−Ru1−Cl1 = 84.604(18).

Scheme 8

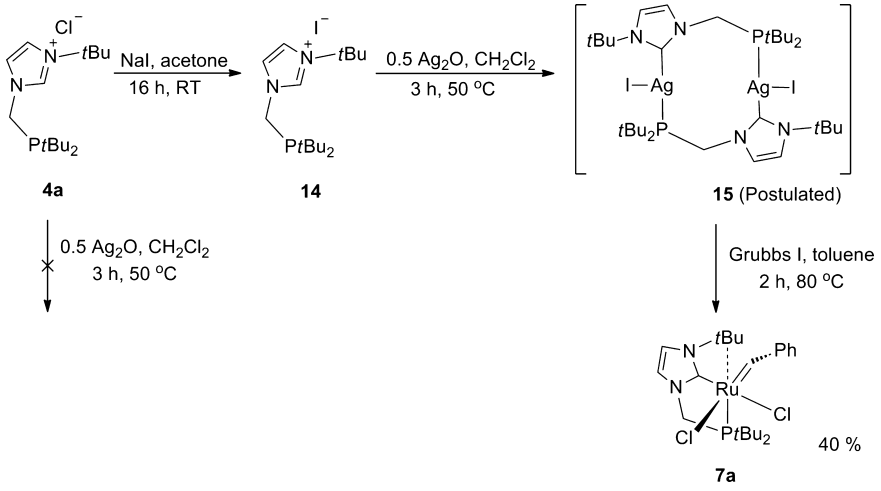

positioned *trans* apparently is sterically unfavorable. Unlike in the case of complex **11**, where the pyridine rings can freely rotate, decreasing the steric hindrance, the bidentate 2,2′-bipyridine ligand imposes a coordination mode that would create significant steric hindrance, if the two chlorides would go *trans*. It is also noteworthy that an attempt to synthesize an adduct complex of type **13** with 6,6′-bis(trifluoromethyl)-2,2′-bipyridine was not successful. This more electron-deficient bipyridine ligand was expected to coordinate less strongly to ruthenium than 2,2′-bipyridine. The steric bulk brought by the CF_3 groups and the lower donor capacity, however, is apparently sufficient to prevent such a coordination. In complex **13** the Ru1−N21 and Ru1−N31 bond lengths are 2.0924(18) and 2.0372(19) Å, respectively. The Ru1−N21 bond that is *trans* to the NHC carbon is the longer one but is shorter than the corresponding bond in **11** (2.169(4) Å), but for **13** a direct comparison of the *trans* influences of the NHC and the tBu_2P arm is of course not possible.

New NHCP-Ruthenium Alkylidene Complexes Using Ruthenium Alkylidene Precursors. Several alkylidene complexes so far have been prepared from different ruthenium alkylidene precursors.[27] For example, the synthesis of the second-generation Grubbs catalysts was achieved by simply exchanging a phosphine ligand from the first-generation catalyst

dx.doi.org/10.1021/om300487r | *Organometallics* 2013, 32, 29−46

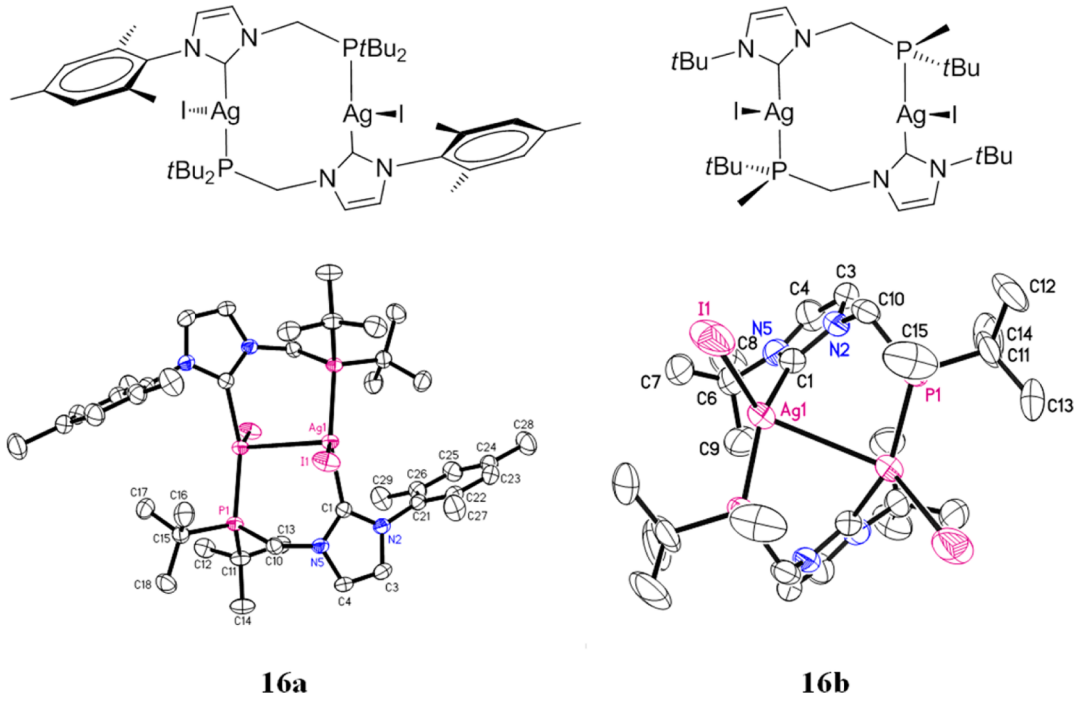

Figure 7. ORTEP plots of **16a** and **16b**. Thermal ellipsoids are at the 50% probability level. Hydrogen atoms are omitted for clarity. Selected bond lengths (Å) and angles (deg) of **16a**: Ag1−P1 = 2.4255(6); Ag1−C1 = 2.164(2); Ag1−I1 = 2.9697; Ag1−Ag1 = 3.1028(4); C1−Ag1−P1 = 150.15(6); C1−Ag1−I1 = 92.38(6); P1−Ag1−I1 = 114.410(16). Selected bond lengths (Å) and angles (deg) of **16b**: Ag1−P1 = 2.367(3); Ag1−C1 = 2.144(11); Ag1−I1 = 2.8980(13); Ag1−Ag1 = 3.1951(17); C1−Ag1−P1 = 151.2(3); C1−Ag1−I1 = 105.5(3); P1−Ag1−I1 = 103.30(8).

Scheme 9

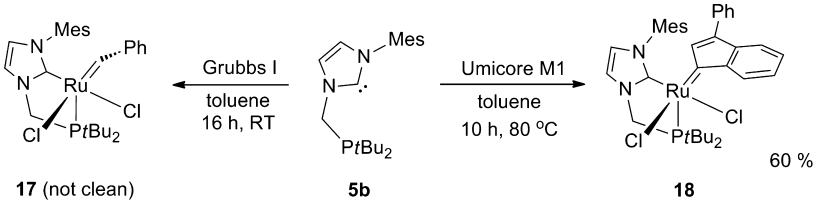

with a stronger σ-donating N-heterocyclic carbene ligand. Therefore, a straightforward rational approach for obtaining ruthenium alkylidene complexes based on ligand **5a** seemed to be its exchange with a phosphine or NHC ligand of a suitable ruthenium alkylidene precursor. Surprisingly, the application of several ruthenium precursors, such as the first-, second-, and third-generation Grubbs catalysts, and the vinyl alkylidene complex $[RuCl_2(PPh_3)_2(=CH-CH=CMe)_2]$[28] with ligand **5a** in different solvents and at variable temperatures did not lead to well-defined reaction products or resulted in the decomposition of either the NHCP ligand or the ruthenium precursor.

As an alternative we investigated the use of silver carbene complexes, which, as described by Wang and Lin,[29] can easily be prepared by deprotonating imidazolium salts with Ag_2O to generate powerful transmetalation reagents. This procedure has already been applied for chiral phosphino-functionalized NHCs and their subsequent transmetalation to rhodium precursors.[30] Interestingly, in the case of **4a** it was necessary to change the counterion to iodide (**14**) in order to achieve full conversion of the imidazolium salt to the desired silver-NHCP complex **15** (Scheme 8). So far, it was not possible to obtain crystals of **15** suitable for X-ray diffraction analysis. Our postulated structure is based upon the structures of related silver complexes bearing ^{Mes}NHCP^{tBu} (**16a**) and a chiral NHCP (^{tBu}NHCP^{tBuMe}) with a *t*Bu and methyl substitution on the phosphorus atom (**16b**), which were synthesized analogously in our group using the corresponding imidazolium iodide salts and Ag_2O. The formation of the silver carbene complex **15** is indicated by the absence of the H1 signal in the ^{1}H NMR spectrum and by a weak signal at 186.1 ppm for the Ag−C carbon in the $^{13}C\{^1H\}$ NMR spectrum. The characteristic signals in the ^{1}H, $^{31}P\{^1H\}$, and $^{13}C\{^1H\}$ NMR spectra are in good accordance with those detected for the analogous silver-NHCP complexes **16a** and **16b** (Figure 7).

The reaction of **15** with the first-generation Grubbs catalyst led to the formation of the ruthenium carbene complex **7a** (Scheme 8) in 40% yield. In contrast to the reaction of phenyldiazomethane with dimer **6** this conversion shows much fewer side products. This transmetalation route is a convenient and less dangerous alternative to the reaction of diazo compounds with dimer **6**.

While our attempts to obtain complexes **7a−e** by direct metalation of ligand **5a** with different ruthenium alkylidene complexes as precursors were not successful, a direct ligand exchange of the first-generation Grubbs catalyst and Umicore M1[31] with the less bulky ligand ^{Mes}NHCP^{tBu} (**5b**) resulted in the formation of the desired products (Scheme 9).

dx.doi.org/10.1021/om300487r | *Organometallics* 2013, 32, 29−46

Complex **17** exhibits in the $^{31}P\{^{1}H\}$ NMR spectrum a singlet at 107.2 ppm and in the ^{1}H NMR spectrum a doublet at 14.97 ppm ($^{3}J_{H,P}$ = 12.5 Hz) of the benzylidene carbon proton. Further spectral data are given in the Experimental Section. **18** exhibits a singlet at 102.4 ppm in the $^{31}P\{^{1}H\}$ NMR spectrum. Its ^{1}H NMR spectrum shows a doublet at 8.94 ppm, which is characteristic for the indenylidene proton of the five-membered ring. The carbene carbon of the alkylidene fragment is observed in the $^{13}C\{^{1}H\}$ NMR at 284.4 ppm as a doublet ($^{2}J_{C,P}$ = 12.1 Hz), and the carbon of the NHC appears at 181.2 ppm as a doublet ($^{2}J_{C,P}$ = 9.1 Hz).

We believe that the reduced steric bulk in **5b** compared to **5a** facilitates the approach of the ruthenium center to the NHC carbene carbon, in contrast to **5a**, with its rotationally invariant bulky *N*-*t*Bu group. On the basis of molecular models of **17** and **18** we assume that the *N*-Mes unit also exerts a stabilizing influence by shielding the empty coordination sites of ruthenium, but so far we have not been able to grow X-ray quality crystals of these ruthenium-carbenes.

SUMMARY

A series of new ruthenium alkylidene complexes (**7a**–**f**) based on stable and isolatable, chelating *N*-phosphinomethyl-functionalized N-heterocyclic carbene ligands were synthesized applying two different methods. A coordinatively unsaturated 16 VE ruthenium dimer (**6**) served as a precursor for the synthesis of these ruthenium alkylidenes utilizing a variety of aryl diazomethanes. In only two of these cases were we able to fully purify and characterize the products (**7b**, **7f**) spectroscopically. Complex **7a** could alternatively be prepared in fair yield by transmetalation from a NHCP silver complex to the first-generation Grubbs catalyst and was isolatable in analytically pure form. Five of the novel ruthenium carbene complexes due to their propensity to crystallize could be characterized by X-ray diffraction, revealing a distorted square pyramidal (or distorted trigonal bipyramidal) geometry, where the two chlorides are positioned *cis* to each other. The direct metalation by ligand substitution was successful only for the reaction of the less bulky free NHCP ligand (**5b**) with Grubbs-type ruthenium alkylidene precursors, which led to the formation of two additional NHCP ruthenium alkylidene complexes (**17** and **18**). A number of other ruthenium complexes bearing phosphine- or pyridine-type ligands were also prepared from complex **6**. Following up the chemistry of cationic bisphosphine ruthenium alkylidene complexes formed by chloride abstraction from *cis*-dichloro alkylidene precursors, which we have reported earlier[2] and which we have shown to be extremely active ROMP catalysts working in ppm catalyst concentrations for various cycloolefins, the investigation of the reactivity of the new alkylidene complexes in halide abstraction reactions and as cationic catalysts in ROMP reactions is under way.

EXPERIMENTAL SECTION

General Procedures. All manipulations were carried out under an atmosphere of dry argon in a glovebox (MBraun) or using standard Schlenk techniques, unless stated otherwise. *N*-*tert*-Butylimidazole,[32] *N*-mesitylimidazole,[33] di-*tert*-butyl(hydroxymethyl)phosphine oxide[14] (**1**), and the phenyldiazomethanes[34] were prepared according to literature procedures. (Trimethylsilyl)diazomethane, the first-generation Grubbs catalyst, and the Umicore M1 catalyst were purchased from Aldrich and used as obtained. Pentane and diethyl ether were distilled over benzophenone sodium-ketyl and stored under argon. Chlorobenzene was distilled over CaH_2. Toluene, hexane, CH_2Cl_2, and THF were dried using an MBraun SPS-800 solvent purification system. Deuterated solvents were purchased from Deutero GmbH or Aldrich. CD_2Cl_2 was stirred over CaH_2 and then degassed three times through freeze–pump–thaw cycles prior to use. Celite was dried at 150 °C in the oven for 1 week. NMR spectra were recorded on a Bruker AC200-300, Bruker ARX250, Bruker DRX300, Bruker DRX500, or Bruker DRX600 spectrometer. The chemical shifts are given in parts per million and are referenced to the deuterated solvent used for ^{1}H and ^{13}C NMR and relative to 85% H_3PO_4 for ^{31}P NMR. Infrared spectra were measured on a Bruker FT-IR Equinox 55 spectrometer in KBr pellets. Mass spectra were recorded on a JEOL JMS-700 or a Finnigan TSQ700 spectrometer and Bruker ApexQe Apollo II FT-ICR instrument. The photoelectron spectrum was measured on a Perkin-Elmer PS18 spectrometer and calibrated with argon. The resolution of the $^{2}P_{3/2}$ argon line is 20 meV. Elemental analyses were performed in the "Mikroanalytisches Laboratorium der Chemischen Institute der Universität Heidelberg".

Di-*tert*-butyl(tosylmethyl)phosphine Oxide (2). Under an air atmosphere in a 500 mL three-necked flask equipped with a dropping funnel, a reflux condenser, and a pressure relief valve, triethylamine (14.2 mL, 105 mmol) was added to a solution of $tBu_2P(O)CH_2OH$ (**1**) (13.40 g, 70 mmol) in THF (210 mL), and the mixture was cooled to −15 °C. A solution of tosyl chloride (14.68 g, 77 mmol) in THF (70 mL) was added dropwise over a period of 40 min. The reaction mixture was allowed to warm to room temperature and stirred overnight. Water (100 mL) and dichloromethane (50 mL) were added, and the layers were separated (brine was added when separation was difficult). The aqueous phase was extracted with dichloromethane (2 × 50 mL). The combined organic phases were washed with brine and dried over $MgSO_4$. The solvent was removed under vacuum, and the residue was purified by column chromatography (SiO_2; dichloromethane–ethanol, 20:1) to give $^{t}Bu_2P(O)CH_2OTs$ (**2**) as a white crystalline solid in 65% (15.6 g) yield. Mp: 73.4–74.0 °C. ^{1}H NMR (300.13 MHz, $CDCl_3$): 7.80 (d, $^{3}J_{H,H}$ = 8.3 Hz, 2H, Ts-*H*), 7.38 (d, $^{3}J_{H,H}$ = 8.3 Hz, 2H, Ts-*H*), 4.26 (d, $^{2}J_{H,P}$ = 6.8 Hz, 2H, PCH_2), 2.46 (s, 3H, Ts-CH_3), 1.28 (d, $^{3}J_{H,P}$ = 13.9 Hz, 18H, $PC(CH_3)_3$). $^{13}C\{^{1}H\}$ NMR (75.48 MHz, $CDCl_3$): 145.7 (s, TsC), 131.1 (s, Ts-*C*), 130.1 (s, Ts-*C*H), 128.2 (s, Ts-*C*H), 61.5 (d, $^{1}J_{C,P}$ = 61 Hz, PCH_2), 35.6 (d, $^{1}J_{C,P}$ = 58 Hz, $P(C(CH_3)_3)_2$), 26.2 (s, $P(C(CH_3)_3)_2$), 21.7 (s, Ts-CH_3). $^{31}P\{^{1}H\}$ NMR (101.26 MHz, $CDCl_3$): 54.3 (s). IR (KBr), ν (cm^{-1}): 750 (s), 814 (s), 977 (s, ν_{C-O}), 998 (s), 1151 (s), 1175 (s, P═O), 1188 (s, P═O), 1371 (s), 1477 (m), 1596 (m), 1917 (w), 2872 (m), 2932 (m), 2971 (m), 3042 (w), 3057 (w). MS (EI^+), *m*/*z* (%): 347.3 (1) $[M+1]^+$, 289.2 (2) $[M - t\text{Bu}]^+$, 233.1 (100) $[M - 2(t\text{Bu}) + 1]^+$, 155.1 (50) $[SO_2 - C_6H_4 - CH_3]^+$, 139.1 (29) $[C_6H_4SO_2]^+$, 91.1 (40) $[C_6H_4CH_3]^+$. Anal. Calcd for $C_{16}H_{27}O_4PS$: C, 55.47; H, 7.86; P, 8.94; S, 9.26. Found: C, 55.49; H, 7.82; P, 8.92; S, 9.10.

3-*tert*-Butyl-1-(di-*tert*-butylphosphinooxymethyl)-imidazolium Tosylate (3a). Into a 50 mL flask equipped with a reflux condenser and a pressure relief valve, **2** (15.6 g, 46 mmol) and *N*-*tert*-butylimidazole (5.7 g, 46 mmol) were added and heated at 100 °C for 4 days. After cooling to room temperature the oily product was dissolved in a minimum amount of dichloromethane and precipitated with diethyl ether. The white solid was washed with diethyl ether and recrystallized from hot THF to give a white crystalline solid as a pure product in 74% (16.0 g) yield. Mp: 192 °C. ^{1}H NMR (250.13 MHz, $CDCl_3$): 10.32 (bs, 1H, NC*H*N), 8.03 (t, $^{3}J_{H,H}$ = 1.7 Hz, 1H, $N(CH)_2N$), 7.80 (d, $^{3}J_{H,H}$ = 8.1 Hz, 2H, Ts-*H*), 7.24 (t, $^{3}J_{H,H}$ = 2.0 Hz, 1H, $N(CH)_2N$), 7.16 (d, $^{3}J_{H,H}$ = 7.6 Hz, 2H, Ts-*H*), 5.21 (d, $^{2}J_{H,P}$ = 4.2 Hz, 2H, PCH_2), 2.35 (s, 3H, Ts-CH_3), 1.69 (s, 9H, $NC(CH_3)_3$), 1.29 (d, $^{3}J_{H,P}$ = 14.3 Hz, 18H, $P(C(CH_3)_3)_2$). $^{13}C\{^{1}H\}$ NMR (75.48 MHz, $CDCl_3$): 143.7 (s, Ts-*C*), 139.1 (s, Ts-*C*), 137.0 (s, NCHN), 128.5 (s, Ts-*C*H), 126.0 (s, Ts-*C*H), 124.4 (s, $N(CH)_2N$), 117.8 (s, $N(CH)_2N$), 60.4 (s, $NC(CH_3)_3$), 41.2 (d, $^{1}J_{C,P}$ = 47.0 Hz, PCH_2), 36.2 (d, $^{1}J_{C,P}$ = 59.0 Hz, $P(C(CH_3)_3)_2$), 29.9 (s, $NC(CH_3)_3$), 26.0 (s, $P(C(CH_3)_3)_2$), 21.2 (s, Ts-CH_3). $^{31}P\{^{1}H\}$ NMR (101.26 MHz, $CDCl_3$): 57.5 (s). IR (KBr), ν (cm^{-1}): 815 (m), 1114 (s), 1131 (s), 1192 (s), 1377 (m), 1398 (m), 1476 (m), 1557 (m), 2871 (w), 2915 (m), 2946 (m), 2979 (w), 3076 (w), 3144 (w), 3196 (w). MS (ESI^+), *m*/*z* (%): 299.43 (100) $[M]^+$, 243.40 (8) $[M - (t\text{Bu}) + 1]^+$. Anal. Calcd for

dx.doi.org/10.1021/om300487r | *Organometallics* 2013, 32, 29–46

$C_{23}H_{39}N_2O_4PS$: C, 58.70; H, 8.35; N, 5.95; P, 6.58; S, 6.81. Found: C, 58.50; H, 8.37; N, 5.94, P, 6.42, S, 6.76.

3-Mesityl-1-(di-*tert*-butylphosphinooxymethyl)imidazolium Tosylate (3b). In a 50 mL two-necked flask equipped with a reflux condenser and a pressure relief valve a mixture of **2** (2.20 g, 6.35 mmol) and *N*-mesitylimidazole (1.18 g, 6.35 mmol) was suspended in dry toluene (10 mL), and then the reaction mixture was heated at 120 °C for 7 days. The solvent was removed on a rotary evaporator, and the yellow residue was dissolved in dichloromethane (5 mL). Diethyl ether (50 mL) was added, resulting in the precipitation of a yellow solid, which was filtered, washed with diethyl ether (3 × 20 mL), and then recrystallized from hot THF. The product was finally dried under vacuum, affording a white solid in 74% (2.5 g) yield. Crystals suitable for X-ray diffraction were obtained by slow evaporation of a concentrated solution of **3b** in chloroform. Mp: 230 °C. ^{1}H NMR (300.13 MHz, $CDCl_3$): 9.67 (s, 1H, NC*H*N), 8.40 (t, $^3J_{H,H}$ = 1.5 Hz, 1H, N(C*H*)$_2$N), 7.70 (d, $^3J_{H,H}$ = 8.0 Hz, 2H, Ts-C*H*), 7.09 (t, $^3J_{H,H}$ = 1.6 Hz, 1H, N(C*H*)$_2$N), 7.06 (d, $^3J_{H,H}$ = 7.7 Hz, 2H, Ts-C*H*), 6.79 (s, 2H, Mes-C*H*), 5.32 (d, $^2J_{H,P}$ = 4.0 Hz, 2H, PCH_2), 2.32 (s, 3H, Mes-*p*-CH_3), 2.29 (s, 3H, Ts-*p*-CH_3), 2.00 (s, 6H, Mes-*o*-CH_3), 1.28 (d, $^3J_{H,P}$ = 14.3 Hz, 18H, P(C(CH_3)$_3$)$_2$). ^{13}C{^{1}H} NMR (75.48 MHz, $CDCl_3$): 143.4 (Ts-*C*), 141.1 (s, Mes-*C*), 139.0 (s, Ts-*C*), 138.4 (s, NCHN), 134.1 (s, Mes-*C*), 130.6 (s, Mes-*C*), 129.7 (s, Mes-CH), 128.4 (s, Ts-CH), 125.8 (s, Ts-CH), 125.5 (s, N(*C*H)$_2$N), 121.9 (s, N(CH)$_2$N), 41.4 (d, $^1J_{C,P}$ = 46.0 Hz, PCH_2), 36.2 (d, $^1J_{C,P}$ = 58.1 Hz, P(*C*(CH$_3$)$_3$)$_2$), 25.9 (s, P(C(*C*H$_3$)$_3$)$_2$), 21.2 (s, Ts-*p*-*C*H$_3$), 21.0 (s, Mes-*p*-*C*H$_3$), 17.3 (s, Mes-*o*-*C*H$_3$). ^{31}P{^{1}H} NMR (101.26 MHz, $CDCl_3$): 59.4 (s). IR (KBr): ν (cm^{-1}) 3078 (m), 3072 (m), 2971 (m), 2954 (m), 1608 (w), 1552 (m), 1479 (m), 1373 (w), 1233 (vs), 1210 (s), 1177 (vs), 1155 (s), 1120 (s), 1034 (s), 1010 (s), 850 (m), 815 (s), 756 (w), 681 (s), 667 (w), 635 (m). MS (ESI$^+$), *m*/*z* (%): 361.24 (100) [M]$^+$. HRMS (ESI$^+$), *m*/*z*: calcd 361.24033; found 361.24037. Anal. Calcd for $C_{28}H_{41}N_2O_4PS$: C, 63.13; H, 7.76; N, 5.26; P, 5.81; S, 6.02. Found: C, 62.94; H, 7.55; N, 5.45; P, 5.77; S, 6.21.

3-*tert*-Butyl-1-(di-*tert*-butylphosphinomethyl)imidazolium Chloride (4a). Into a 2 L four-necked flask equipped with a stopcock olive tap, a reflux condenser with a pressure relief valve, and a pressure-equalizing dropping funnel was added phosphine oxide **3a** (9.30 g, 19.8 mmol), and the mixture was then dissolved in dry chlorobenzene (280 mL) by heating to reflux temperature. The temperature was then maintained at 120 °C, and $HSiCl_3$ (35.0 mL, 251 mmol, 17-fold excess) was added dropwise. When the addition was complete, the reaction mixture was heated at 120 °C overnight. If necessary, an additional 5 equiv of $HSiCl_3$ was added, and the mixture was stirred until a full conversion was detected by ^{31}P NMR spectroscopy. After cooling to room temperature the volatiles were removed under vacuum and the residue was extracted with dichloromethane (3 × 10 mL), filtered, and dried again. The residue was washed with diethyl ether (3 × 20 mL) and finally dried under vacuum, affording a white solid in 60% (3.80 g) yield. ^{1}H NMR (300.13 MHz, CD_2Cl_2): 10.82 (s, 1H, NC*H*N), 7.60 (d, $^3J_{H,H}$ = 1.3 Hz, 1H, N(C*H*)$_2$N), 7.25 (t, $^3J_{H,H}$ = 1.8 Hz, 1H, N(C*H*)$_2$N), 4.80 (s, 2H, PCH_2), 1.71 (s, 9H, NC(CH_3)$_3$), 1.20 (d, $^3J_{H,P}$ = 12.0 Hz, 18 H, P(C(CH_3)$_3$)$_2$). ^{13}C{^{1}H} NMR (125.78 MHz, CD_2Cl_2): 137.7 (s, NCHN), 122.7 (s, N(CH)$_2$N), 119.2 (s, N(CH)$_2$N), 45.2 (d, $^1J_{C,P}$ = 24 Hz, PCH_2), 32.6 (d, $^1J_{C,P}$ = 19 Hz, P(*C*(CH$_3$)$_3$)$_2$), 30.3 (s, NC(*C*H$_3$)$_3$), 29.7 (d, $^2J_{C,P}$ = 14 Hz, P(C(*C*H$_3$)$_3$)$_2$), 26.4 (s, NC(*C*H$_3$)$_3$). ^{31}P{^{1}H} NMR (202.47 MHz, CD_2Cl_2): 29.2 (s). IR (KBr), ν (cm^{-1}): 1370 (w), 1380 (w), 1469 (w), 1555 (m), 2862 (m), 2895 (m), 2937 (m), 2977 (m), 3049 (m), 3080 (w), 3134 (w). MS (ESI$^+$), *m*/*z* (%): 283.5 (70) [M]$^+$, 159.5 (100) [CH_2P*t*Bu]$^+$.

3-Mesityl-1-(di-*tert*-butylphosphinomethyl)imidazolium Chloride (4b). Into a 500 mL four-necked flask equipped with a dropping funnel, a reflux condenser, a stopcock olive tap, and a pressure relief valve was added **3a** (2.00 g, 3.75 mmol), and the system was put under argon flow. Dry chlorobenzene (70 mL) was then added, and the solution was heated to 80 °C. At this temperature, $HSiCl_3$ (7.5 mL, 75 mmol, 20 equiv) was added dropwise and the reaction mixture was stirred for 24 h. An additional 7 equiv of $HSiCl_3$ (2.5 mL, 25 mmol) was then added, and the reaction mixture was heated for 24 h at 80 °C. The volatiles were removed under vacuum, and the residue was extracted with dichloromethane (3 × 10 mL), filtered, and dried again. The residue was washed with diethyl ether (3 × 20 mL) and pentane (20 mL) and finally dried under vacuum, affording a white solid in 94% (1.34 g) yield. Crystals suitable for X-ray analysis were obtained by slow condensation of pentane into a saturated solution of **4b** in $CHCl_3$. Mp: 235 °C (dec). ^{1}H NMR (500.13 MHz, $CDCl_3$): 11.04 (s, 1H, NC*H*N), 8.23 (s, 1H, N(C*H*)$_2$N), 7.15 (s, 1H, N(C*H*)$_2$N), 6.97 (s, 2H, Mes-C*H*), 5.44 (s, 2H, PCH_2), 2.31 (s, 3H, Mes-*p*-CH_3), 2.02 (s, 6H, Mes-*o*-CH_3), 1.32 (d, $^3J_{H,P}$ = 12.9 Hz, 18H, P(C(CH_3)$_3$)$_2$). ^{13}C{^{1}H} NMR (125.77 MHz, $CDCl_3$): 141.2 (s, Mes-*C*), 139.4 (s, NCHN), 134.0 (s, Mes-*C*), 130.7 (s, Mes-*C*), 129.8 (Mes-CH), 123.5 (s, N(CH)$_2$N), 122.6 (s, N(CH)$_2$N), 43.8 (d, $^1J_{C,P}$ = 14.2 Hz, PCH$_2$), 32.7 (d, $^1J_{C,P}$ = 12.5 Hz, P(*C*(CH$_3$)$_3$)$_2$), 29.1 ($^2J_{C,P}$ = 11.0 Hz, P(C(*C*H$_3$)$_3$)$_2$), 21.0 (Mes-*p*-*C*H$_3$), 17.5 (Mes-*o*-*C*H$_3$). ^{31}P{^{1}H} NMR (101.26 MHz, $CDCl_3$): 33.3 (s). IR (KBr), ν (cm^{-1}): 2950 (vs), 2864 (vs), 2360 (w), 1608 (w), 1546 (m), 1471 (s), 1369 (m), 1261 (w), 1206 (s), 1161 (s), 1102 (m), 1039 (m), 968 (w), 855 (w), 811 (m), 749 (w), 669 (w). MS (ESI$^+$), *m*/*z* (%): 725.46 (45) [2M − Cl]$^+$, 345.25 (100) [M]$^+$. HRMS (ESI$^+$): *m*/*z* calcd 725.46023, 345.24541; found 725.46011, 345.24547.

3-*tert*-Butyl-1-(di-*tert*-butylphosphinomethyl)imidazol-2-ylidene, ^{tBu}NHCP^{tBu} (5a). Into a 10 mL Schlenk flask **4a** (100 mg, 0.31 mmol) was suspended in 6 mL of THF, and KO*t*Bu (41.0 mg, 0.35 mmol, 1.1 equiv) was added in portions. The reaction mixture was stirred for 2 h, and all volatiles were removed under vacuum. The residue was extracted with pentane (5 × 10 mL), and the filtrate was dried under vacuum, affording a white solid in 72% (63 mg) yield. **5a** is stored in the glovebox at −20 °C. Mp: 79 °C. Crystals suitable for X-ray analysis were obtained from a saturated solution of **5a** in pentane at −20 °C. ^{1}H NMR (300.13 MHz, C_6D_6): 7.21 (d, *J* = 1.4 Hz, 1H, N(C*H*)$_2$N), 6.74 (s, 1H, N(C*H*)$_2$N), 4.49 (d, $^2J_{H,P}$ = 2.1 Hz, 2H, PCH_2), 1.49 (s, 9H, NC(CH_3)$_3$), 1.08 (d, $^3J_{H,P}$ = 10.8 Hz, 18H, PC(CH_3)$_3$). ^{13}C{^{1}H} NMR (75.48 MHz, C_6D_6): 215.2 (s, NCN), 118.8 (d, *J* = 9 Hz, N(CH)$_2$N), 116.3 (s, N(CH)$_2$N), 56.1 (s, NC(CH$_3$)$_3$), 47.0 (d, $^1J_{C,P}$ = 20 Hz, PCH$_2$), 32.0 (d, $^1J_{C,P}$ = 22 Hz, PC(CH$_3$)$_3$), 31.8 (s, NC(*C*H$_3$)$_3$), 30.1 (d, $^2J_{C,P}$ = 13 Hz, PC(*C*H$_3$)$_3$). ^{31}P{^{1}H} NMR (121.49 MHz, C_6D_6): 23.5 (s). IR (KBr), ν (cm^{-1}): 735 (s), 809 (m), 822 (m), 1019 (w), 1099 (m), 1127 (m), 1204 (m), 1230 (s), 1365 (s), 1391 (s), 1463 (s), 1475 (s), 1551 (w), 2859 (s), 2896 (s), 2941 (s), 2973 (s), 3051 (s). MS (LIFDI), *m*/*z* (%): 283.3 (100) [M + 1]$^+$.

3-Mesityl-1-(di-*tert*-butylphosphinomethyl)imidazol-2-ylidene, ^{Mes}NHCP^{tBu} (5b). **4b** (305 mg, 0.80 mmol) was suspended in THF (10 mL); then KO*t*Bu (108 mg, 0.96 mmol, 1.2 equiv) was added in portions. The reaction mixture was stirred for 2 h at room temperature, and then all volatiles were removed under vacuum. The residue was extracted with pentane (3 × 8 mL), filtered through Celite, and dried under vacuum, affording a yellow, viscous oil in 65% (180 mg) yield. The oil was stored under argon at −20 °C. ^{1}H NMR (300.13 MHz, THF-d_8): 7.31 (d, $^3J_{H,H}$ = 1.5 Hz, 1H, N(C*H*)$_2$N), 6.87 (s, 2H, Mes-C*H*), 6.87 (d, $^3J_{H,H}$ = 1.5 Hz, 1H, N(C*H*)$_2$N), 4.55 (d, $^2J_{H,P}$ = 1.6 Hz, 2H, PCH_2), 2.28 (s, 3H, Mes-*p*-CH_3), 1.96 (s, 6H, Mes-*o*-CH_3), 1.21 (d, $^3J_{H,P}$ = 11.0 Hz, 18H, P(C(CH_3)$_3$)$_2$). ^{13}C{^{1}H} NMR (75.48 MHz, THF-d_8): 219.5 (s, NCN), 141.7 (s, Mes-*C*), 137.6 (s, Mes-*C*), 136.0 (s, Mes-*C*), 129.4 (s, Mes-CH), 121.7 (s, N(CH)$_2$N), 119.8 (s, N(CH)$_2$N), 46.9 (d, $^1J_{C,P}$ = 20.7 Hz, PCH$_2$), 32.4 (d, $^1J_{C,P}$ = 21.8 Hz P(*C*(CH$_3$)$_3$)$_2$), 20.2 (d, $^2J_{C,P}$ = 13.2 Hz, P(C(*C*H$_3$)$_3$)$_2$), 21.2 (s, Mes-*p*-*C*H$_3$), 18.3 (s, Mes-*o*-*C*H$_3$). ^{31}P{^{1}H} NMR (101.26 MHz, THF-d_8): 26.5 (s). MS (LIFDI), *m*/*z* (%): 345.12 (100) [M + 1]$^+$.

[RuCl(^{tBu}NHCP^{tBu})$_2$-(μ-Cl)$_2$] (6). Method a: In a glovebox a 20 mL glass autoclave was charged with [$RuCl_2$(COD)]$_n$ (430 mg, 1.54 mmol Ru), **5a** (475 mg, 1.68 mmol), and dry THF (15 mL). The vessel was pressurized with hydrogen (18 bar), and the reaction mixture was stirred at 80 °C for 72 h, after which the hydrogen pressure had dropped to 12 bar. The autoclave was cooled to room temperature, and the pressure was released. The formed slurry was allowed to settle, and the dark brown solution was decanted. The green solid was washed with diethyl ether (4 × 8 mL) and dried under vacuum,

dx.doi.org/10.1021/om300487r | *Organometallics* 2013, 32, 29−46

resulting in 79% (553 mg) yield. ^{1}H NMR (600.13 MHz, CD_2Cl_2), first set of signals: 7.25 (d, $^3J_{H,H}$ = 1.9 Hz, 2H, N(C*H*)$_2$N), 7.20 (d, $^3J_{H,H}$ = 2.1 Hz, 2H, N(C*H*)$_2$N), 4.14−4.17 (m, 2H, PC*H*$_2$), 3.78−3.81 (m, 2H, PC*H*$_2$), 1.85 (s, 18H, NC(C*H*$_3$)$_3$), 1.37 (d, $^3J_{H,P}$ = 13.6 Hz, 18H, P(C(C*H*$_3$)$_3$)$_2$), 1.16 (d, $^3J_{H,P}$ = 12.8 Hz, 18H, P(C(C*H*$_3$)$_3$)$_2$); second set of signals: 7.23 (d, $^3J_{H,H}$ = 2.1 Hz, 2H, N(C*H*)$_2$N), 7.17 (d, $^3J_{H,H}$ = 2.1 Hz, 2H, N(C*H*)$_2$N), 4.18−4.21 (m, 2H, PC*H*$_2$), 3.79−3.83 (m, 2H, PC*H*$_2$), 1.83 (s, 18H, NC(C*H*$_3$)$_3$), 1.51 (d, $^3J_{H,P}$ = 13.6 Hz, 18H, P(C(C*H*$_3$)$_3$)$_2$), 1.29 (d, $^3J_{H,P}$ = 12.7 Hz, 18H, P(C(C*H*$_3$)$_3$)$_2$). ^{13}C{^{1}H} NMR (150.90 MHz, CD_2Cl_2), first set of signals: 191.3 (d, $^2J_{C,P}$ = 12.7 Hz, NCN), 119.3 (s, N(CH)$_2$N), 119.3 (d, $^3J_{C,P}$ = 8.0 Hz, N(CH)$_2$N), 58.4 (s, NC(CH$_3$)$_3$), 46.6 (d, $^1J_{C,P}$ = 27.2 Hz, PCH$_2$), 39.8 (d, $^1J_{C,P}$ = 18.4 Hz, P(C(CH$_3$)$_3$)$_2$), 38.9 (d, $^1J_{C,P}$ = 18.7 Hz, P(C(CH$_3$)$_3$)$_2$), 33.4 (s, NC(CH$_3$)$_3$), 31.1 (d, $^2J_{C,P}$ = 2.5 Hz, P(C(CH$_3$)$_3$)$_2$), 29.6 (bs, P(C(CH$_3$)$_3$)$_2$); second set of signals, 191.0 (d, $^2J_{C,P}$ = 13.2 Hz, NCN), 119.4 (d, $^3J_{C,P}$ = 7.4 Hz, N(CH)$_2$N), 119.1 (s, N(CH)$_2$N), 58.2 (s, NC(CH$_3$)$_3$), 46.4 (d, $^1J_{C,P}$ = 27.0 Hz, PCH$_2$), 37.3 (d, $^1J_{C,P}$ = 21.5 Hz, P(C(CH$_3$)$_3$)$_2$), 37.1 (d, $^1J_{C,P}$ = 21.2 Hz, P(C(CH$_3$)$_3$)$_2$), 33.4 (s, NC(CH$_3$)$_3$), 31.5 (d, $^1J_{C,P}$ = 2.5 Hz, P(C(CH$_3$)$_3$)$_2$), 29.7 (d, $^1J_{C,P}$ = 2.5 Hz, P(C(CH$_3$)$_3$)$_2$). ^{31}P{^{1}H} NMR (242.94 MHz, CD_2Cl_2): 132.3 (s), 130.5 (s). IR (KBr), ν (cm^{-1}): 3132 (w), 2962 (s), 1630 (m), 1475 (m), 1362 (s), 1231 (s), 1046 (m, 682 (m). MS (FAB$^+$), *m*/*z* (%): 910.1 (35) [M]$^+$, 454.0 (100) [1/2M]$^+$, 383.1 (90) [Ru(NHCP)]$^+$. HRMS (FAB$^+$), *m*/*z*: calcd for $C_{32}H_{62}Cl_4N_4P_2Ru_2$ 908.1291; found 908.1349. Anal. Calcd for $C_{32}H_{62}Cl_4N_4P_2Ru_2$: C, 42.29; H, 6.88; N, 6.17; P, 6.82. Found: C, 42.12; H, 6.92; N, 6.30; P, 6.80.

Method b: In the glovebox a 10 mL glass autoclave was charged with [RuCl$_2$(cymene)]$_2$ (100 mg, 0.163 mmol) and toluene (5 mL). Ligand **5a** (96.8 mg; 0.343 mmol) was added, slowly leading to a color change from orange to green. Then the reaction mixture was heated at 80 °C for 20 h. After cooling to room temperature pentane (10 mL) was added for a better precipitation. The brown solution was decanted, and the green residue was washed with pentane (3 × 10 mL). The green solid was dried under vacuum, affording a 68% (100 mg) yield. Mp: 192 °C. ^{1}H NMR (250.1 MHz, CD_2Cl_2): 7.28 (s, 2H, N(C*H*)$_2$N), 7.14 (d, $^3J_{H,H}$ = 11.8 Hz, 2H, N(C*H*)$_2$N), 4.22 (bs, 2H, C*H*$_2$P), 3.68 (d, $^2J_{H,H}$ = 11.9 Hz, 2H, C*H*$_2$P), 1.76 (s, 12H, NC(C*H*$_3$)$_2$), 1.45 (s, 6H, NC(C*H*$_3$)$_2$), 1.42−1.00 (m, 36H, P(C-(C*H*$_3$)$_3$)$_2$). ^{31}P{^{1}H} NMR (101.2 MHz, CD_2Cl_2): 133.5 (s), 131.7 (s). MS (FAB$^+$), *m*/*z* (%): 909.0 (20) [M]$^+$, 873.0 (10) [M − Cl]$^+$, 454.1 (70) [1/2M]$^+$, 383.2 (60) [1/2M − 2Cl]$^+$. Anal. Calcd for $C_{32}H_{62}Cl_4N_4P_2Ru_2$: C, 42.29; H, 6.88; N, 6.17. Found: C, 42.70; H 6.90; N, 6.12.

[RuCl$_2$(*t*BuNHCP*t*Bu)(benzylidene)] (7a). Method a: Into an NMR tube were added complex **6** (10.0 mg, 11 μmol), phenyldiazomethane (5.0 mg, 42 μmol), and CD_2Cl_2 (0.5 mL), affording a green solution. Complex **7a** was contaminated with byproducts and therefore could not be fully characterized. Mp: 152 °C (dec). Selected spectral data: ^{31}P{^{1}H} NMR: (101.26 MHz, THF-d_8): 133.4 (s, P(C(CH$_3$)$_3$)$_2$). ^{1}H NMR (250.13 MHz, THF-d_8): 14.82 (d, $^3J_{H,P}$ = 8.6 Hz, 1H, Ru=C*H*). MS (FAB$^+$), *m*/*z* (%): 509.2 [M − Cl]$^+$ (100), 454.1 [RuCl$_2$(NHCP)]$^+$ (15), 383.1 [Ru(NHCP)]$^+$ (35). HRMS (FAB$^+$), *m*/*z*: calcd for $C_{23}H_{37}ClN_2PRu$ 509.1426; found 509.1446. Method b: Into a Schlenk tube were added complex **15** (100 mg, 193 μmol) and first-generation Grubbs catalyst (159 mg, 193 μmol) and suspended in toluene (5 mL). The slurry was stirred under heating at 80 °C for 2 h, resulting in a color change from violet to brown and in a precipitated green solid. The slurry was filtered through a cotton and Celite pad and washed with toluene (5 mL). The green solid on the pad was dissolved with dichloromethane (10 mL), leaving a violet material. The filtrate was dried under vacuum, affording a green solid in 40% (42 mg) yield. ^{1}H NMR (600.13 MHz, CD_2Cl_2): 14.97 (d, $^3J_{H,P}$ = 8.2 Hz, 1H, Ru=C*H*), 8.40 (d, $^3J_{H,H}$ = 7.7 Hz, 2H, Ar), 7.68 (t, $^3J_{H,H}$ = 7.4 Hz, 1H, Ar), 7.45 (t, $^3J_{H,H}$ = 7.8 Hz, 2H, Ar), 7.36 (d, $^3J_{H,H}$ = 1.9 Hz, 1H, N(C*H*)$_2$N), 7.05 (d, $^3J_{H,H}$ = 1.9 Hz, 1H, N(C*H*)$_2$N), 4.42 (d, $^2J_{H,P}$ = 5.8 Hz, 2H, PC*H*$_2$), 1.48 (d, $^3J_{H,P}$ =14.3 Hz, 9H, PC(C*H*$_3$)$_3$), 1.19 (s, 9H, NC(C*H*$_3$)$_3$), 1.13 (d, $^3J_{H,P}$ = 14.6 Hz, 9H, PC(C*H*$_3$)$_3$). ^{13}C{^{1}H} NMR (150.90 MHz, CD_2Cl_2): 295.4 (d, $^2J_{C,P}$ = 15.9 Hz, Ru=CH), 178.8 (d, $^2J_{C,P}$ = 10.3 Hz, NCN), 151.0 (d, $J_{C,P}$ = 1.9 Hz, Ar) 131.6 (bs, Ar), 131.3 (s, Ar), 129.6 (s, Ar), 120.9 (s, N(CH)$_2$N), 119.6 (d, $J_{C,P}$ = 8.8 Hz, N(CH)$_2$N), 59.8 (s, NC(CH$_3$)$_3$), 44.2 (d, $^1J_{C,P}$ = 27.1 Hz, PCH$_2$), 38.74 (d, $^1J_{C,P}$ = 22.0 Hz, PC(CH$_3$)$_3$), 37.2 (d, $^1J_{C,P}$ = 24.0 Hz, PC(CH$_3$)$_3$), 32.0 (s, NC(CH$_3$)$_3$), 29.3 (d, $^2J_{C,P}$ = 3.3 Hz, PC(CH$_3$)$_3$), 29.1 (d, $^2J_{C,P}$ = 2.0 Hz, PC(CH$_3$)$_3$). ^{31}P{^{1}H} NMR (242.94 MHz, CD_2Cl_2): 131.4 (s). HRMS (FAB$^+$), *m*/*z*: calcd for $C_{23}H_{37}ClN_2PRu$ 509.1430; found 509.1440. Anal. Calcd for $C_{23}H_{37}Cl_2N_2PRu$: C, 50.73; H, 6.85; N, 5.14. Found: C, 45.90; H, 6.44; N, 4.36. Analysis: The results obtained from three samples suit an additional molecule of dichloromethane per molecule in the solid. Anal. Calcd for $C_{23}H_{37}Cl_2N_2PRu{\cdot}CH_2Cl_2$: C, 45.80; H, 6.25; N, 4.45.

[RuCl$_2$(*t*BuNHCP*t*Bu)(4-bromobenzylidene)] (7b). Complex **6** (100 mg, 110 μmol) was suspended in dichloromethane (8 mL). Freshly prepared *p*-bromophenyldiazomethane (70.0 mg, 355 μmol) was dissolved in dichloromethane (1.5 mL) and added at 0 °C via syringe pump (∼2 mL/h). After complete addition, the reaction mixture was warmed to room temperature, filtered, and concentrated to ca. 0.5 mL. Diethyl ether (5 mL) was added, resulting in precipitation of a solid, and the supernatant was decanted. The resulting green solid was washed with diethyl ether (2 × 5 mL), and the residue was dried under vacuum, affording a green solid in 65% (89 mg) yield. ^{1}H NMR (600.13 MHz, CD_2Cl_2): 14.86 (d, $^3J_{H,P}$ = 8.4 Hz, 1H, Ru=C*H*), 8.32 (bs, 2H, Ar), 7.58 (d, $^3J_{H,H}$ = 8.4 Hz, 2H, Ar), 7.37 (s, 1H, N(C*H*)$_2$N), 7.07 (s, 1H, N(C*H*)$_2$N), 4.45 (dd, $^2J_{H,H}$ = 14.1 Hz, $^2J_{H,P}$ = 10.1 Hz, 1H, PC*H*$_2$), 4.39 (dd, $^2J_{H,H}$ = 14.1 Hz, $^2J_{H,P}$ = 2.8 Hz, 1H, PC*H*$_2$), 1.48 (d, $^3J_{H,P}$ = 14.3 Hz, 9H, P(C(C*H*$_3$)$_3$)$_2$), 1.19 (s, 9H, NC(C*H*$_3$)$_3$), 1.11 (d, $^3J_{H,P}$ = 14.7 Hz, 9H, P(C(C*H*$_3$)$_3$)$_2$). ^{13}C{^{1}H} NMR (150.90 MHz, CD_2Cl_2): 292.2 (d, $^2J_{C,P}$ = 15.7 Hz, Ru=CH), 178.3 (d, $^2J_{C,P}$ = 10.0 Hz, NCN), 149.5 (d, *J* = 1.6 Hz, Ar), 132.9 (s, Ar), 132.8 (bs, Ar), 125.9 (s, Ar), 121.0 (s, N(CH)$_2$N), 119.7 (d, $^3J_{C,P}$ = 8.4 Hz, N(CH)$_2$N), 59.9 (s, NC(CH$_3$)$_3$), 44.3 (d, $^1J_{C,P}$ = 27.0 Hz, PCH$_2$), 38.4 (d, $^1J_{C,P}$ = 21.8 Hz, P(C(CH$_3$)$_3$)$_2$), 37.2 (d, $^1J_{C,P}$ = 23.8 Hz, P(C(CH$_3$)$_3$)$_2$), 32.1 (s, NC(CH$_3$)$_3$), 29.3 (d, $^2J_{C,P}$ = 2.7 Hz, P(C(CH$_3$)$_3$)$_2$), 29.1 (d, $^2J_{C,P}$ = 1.4 Hz, P(C(CH$_3$)$_3$)$_2$); contains traces of Et$_2$O and 4,4′-dibromostilbene. ^{31}P{^{1}H} NMR (242.94 MHz, CD_2Cl_2): 131.2 (s). IR (KBr), ν (cm^{-1}): 2955 (s), 1571 (m), 1479 (s), 1368 (m), 1178 (s), 1070 (m), 1007 (m), 871 (m), 808 (m), 694 (w), 508 (m). MS (FAB$^+$), *m*/*z* (%): 624.1 [M]$^+$ (1), 589.1 [M − Cl]$^+$ (100). HRMS (FAB$^+$), *m*/*z* (%): calcd for $C_{23}H_{36}BrCl_2N_2PRu$ 622.0220; found 622.0205.

[RuCl$_2$(*t*BuNHCP*t*Bu)(4-(trifluoromethyl)benzylidene)] (7c). Complex **6** (10 mg, 11 μmol) was suspended in dichloromethane (5 mL), and then (4-(trifluoromethyl)diazomethane (7.0 mg, 38 μmol) was added to the mixture as a solid. The reaction mixture was stirred for 1.5 h at room temperature, showing a slight evolution of a gas. The resulting green solution was filtered and concentrated to ca. 1 mL, and the product was precipitated by addition of pentane (2 mL). The precipitate was washed again with pentane (2 mL) and dried under vacuum, affording a greenish-brown solid. The yield could not be determined as a result of contamination with byproducts and with *E*/*Z*-stilbene, and a full spectral characterization could not be achieved. ^{1}H NMR (600.13 MHz, CD_2Cl_2): 15.10 (d, $^3J_{H,P}$ = 8.4 Hz, 1H, Ru=C*H*), 8.54 (d, $^3J_{H,H}$ = 7.4 Hz, 2H, Ar), 7.69 (d, $^3J_{H,H}$ = 8.1 Hz, 2H, Ar), 7.38 (s, 1H, N(C*H*)$_2$N), 7.09 (s, 1H, N(C*H*)$_2$N), 4.45−4.52 (m, 1H, PC*H*$_2$), 4.40−4.44 (m, 1H, PC*H*$_2$), 1.49 (d, $^3J_{H,P}$ = 14.3 Hz, 9H, P(C(C*H*$_3$)$_3$)$_2$), 1.19 (s, 9H, NC(C*H*$_3$)$_3$), 1.12 (d, $^3J_{H,P}$ = 14.9 Hz, 9H, P(C(C*H*$_3$)$_3$)$_2$). ^{13}C{^{1}H} NMR (150.90 MHz, CD_2Cl_2): 291.6 (d, $^2J_{C,P}$ = 4.6 Hz, Ru=CH), 177.6 (d, $^2J_{C,P}$ = 9.4 Hz, NCN), 152.2 (bs, Ar), 131.2 (s, Ar), 129.7 (s, Ar), 126.6 (bs, Ar), 126.2 (bs, CF_3), 121.2 (s, N(CH)$_2$N), 119.9 (d, $^3J_{C,P}$ = 8.3 Hz, N(CH)$_2$N), 60.0 (s, NC(CH$_3$)$_3$), 44.5 (d, $^1J_{C,P}$ = 26.6 Hz, PCH$_2$), 38.3 (d, $^1J_{C,P}$ = 21.7 Hz, P(C(CH$_3$)$_3$)$_2$) 37.1 (d, $^1J_{C,P}$ = 24.0 Hz, P(C(CH$_3$)$_3$)$_2$), 32.1 (s, NC(CH$_3$)$_3$), 29.3 (bs, P(C(CH$_3$)$_3$)$_2$), 29.0 (bs, P(C(CH$_3$)$_3$)$_2$). ^{31}P{^{1}H} NMR (242.94 MHz, CD_2Cl_2): 130.7 (s). ^{19}F NMR (376.27 MHz, CD_2Cl_2, RT): −63.7 (s, CF_3). MS (FAB$^+$), *m*/*z* (%): 612.5 [M]$^+$ (2), 577.2 [M − Cl]$^+$ (100), 454.1 [RuCl$_2$(NHCP)]$^+$ (8), 383.2 [Ru(NHCP)]$^+$ (10). HRMS (FAB$^+$), *m*/*z* (%): calcd for $C_{24}H_{36}Cl_2F_3N_2PRu$ 577.1300; found 577.1313.

dx.doi.org/10.1021/om300487r | *Organometallics* 2013, 32, 29−46

[RuCl$_2$($^{t\mathrm{Bu}}$NHCP$^{t\mathrm{Bu}}$)(4-nitrobenzylidene)] (7d). Complex **6** (10 mg, 11 μmol) was suspended in dichloromethane (4 mL), and to it was added (4-nitrophenyl)diazomethane (4.0 mg, 25 μmol) as a solid. The reaction mixture was stirred for 1.5 h at room temperature while observing a slight evolution of a gas. The resulting green solution was concentrated to 1 mL, and to it was added pentane (2 mL), resulting in the precipitation of a green solid. The supernatant was decanted, and the solid was washed with pentane (2 mL). The residue was dried under vacuum, affording a brownish-green solid. The yield could not be determined as a result of contamination, and a full spectral characterization could not be achieved. ^{1}H NMR (250.14 MHz, CD_2Cl_2): 15.10 (d, $^3J_{H,P}$ = 8.8 Hz, 1H, Ru=C*H*), 8.57 (d, $^3J_{H,H}$ = 8.8 Hz, 2H, Ar), 7.10 (d, $^3J_{H,H}$ = 2.2 Hz, 1H, N(C*H*)$_2$N), 4.37−4.58 (m, 2H, PC*H*$_2$), 1.48 (d, $^3J_{H,P}$ = 14.5 Hz, 9H, P(C(C*H*$_3$)$_3$)$_2$), 1.18 (s, 9H, NC(C*H*$_3$)$_3$), 1.12 (d, $^3J_{H,P}$ = 15.1 Hz, 9H, P(C(C*H*$_3$)$_3$)$_2$); as a result of contamination missing signals are probably covered, and signals at around 7.38 (1H, N(C*H*)$_2$N), 7.69 (2H, Ar) can be assigned. ^{31}P{^{1}H} NMR (101.26 MHz, CD_2Cl_2): 131.2 (s). MS (FAB$^+$), *m*/*z* (%): 554.2 [M − Cl]$^+$ (100), 454.1 [RuCl$_2$(NHCP)]$^+$ (25). HRMS (FAB$^+$), *m*/*z* (%): calcd for $C_{23}H_{36}ClN_3O_2PRu$ 554.1277; found 554.1403.

[RuCl$_2$($^{t\mathrm{Bu}}$NHCP$^{t\mathrm{Bu}}$)(4-methylbenzylidene)] (7e). Complex **6** (40.0 mg, 44 μmol) was suspended in chloroform (3.5 mL); then (4-tolyl)diazomethane (30.0 mg, 230 μmol) was added. The reaction mixture was stirred for 1.5 h at room temperature and then for additional 1.5 h at 60 °C, leading to the slight evolution of a gas. The resulting brownish-green solution was concentrated to ca. 0.7 mL, and pentane (2 mL) was added, resulting in the product precipitation. The solid was washed with pentane (2 mL) and dried under vacuum, affording a brownish-green solid. The yield could not be determined as a result of contamination, and a full spectral characterization could not be achieved. Selected spectral data: ^{1}H NMR (500.13 MHz, CD_2Cl_2): 14.85 (m, 1H, Ru=C*H*). ^{31}P{^{1}H} NMR (101.26 MHz, CD_2Cl_2): 133.0 (s). IR (KBr), ν (cm^{-1}): 2962 (s), 1951 (s), 1597 (m), 1477 (s), 1369 (s), 1233 (m), 1178 (s), 1019 (m), 810 (m), 691 (w), 506 (m). MS (FAB$^+$): NBA-matrix, *m*/*z* (%), 523.2 [M − Cl]$^+$ (70), 454.1 [RuCl$_2$(NHCP)]$^+$ (15), 383.2 [Ru(NHCP)]$^+$ (55), 208.1 [dimethylstilbene] (100). HRMS (FAB$^+$), *m*/*z* (%): calcd for $C_{24}H_{39}ClN_2PRu$ 523.1583; found 523.1524.

[RuCl$_2$($^{t\mathrm{Bu}}$NHCP$^{t\mathrm{Bu}}$)(=CH-SiMe$_3$)] (7f). Complex **6** (76.0 mg, 110 μmol) was suspended in dichloromethane (8 mL), and then (trimethylsilyl)diazomethane (180 μL, 2 M in THF, 350 μmol) was added slowly via syringe. The reaction mixture was stirred for 30 min at room temperature, and then it was heated at 60 °C for 2.5 h, resulting in the formation of a brown solid. The solution was then concentrated to 0.5 mL, and pentane (3 mL) was added for complete product precipitation. The greenish-brown solution was decanted, and the brown solid was washed with pentane (4 × 2 mL). The product was dried under vacuum, affording a brown solid in 60% (54 mg) yield. ^{1}H NMR (600.13 MHz, CD_2Cl_2): 18.93 (d, $^3J_{H,P}$ = 3.4 Hz, 1H, Ru=C*H*), 7.34 (d, $^3J_{H,H}$ = 2.1 Hz, N(C*H*)$_2$N), 7.06 (d, $^3J_{H,H}$ = 2.1 Hz, 1H, N(C*H*)$_2$N), 4.40 (dd, $^2J_{H,H}$ = 14.0 Hz, $^2J_{H,P}$ = 10.3 Hz, 2H, PC*H*$_2$), 4.29 (dd, $^2J_{H,H}$ = 14.0 Hz, $^2J_{H,P}$ = 3.2 Hz, 2H, PC*H*$_2$), 1.41 (d, $^3J_{H,P}$ = 14.2 Hz, 9H, P(C(C*H*$_3$)$_3$)$_2$), 1.31 (s, 9H, NC(C*H*$_3$)$_3$), 1.07 (d, $^3J_{H,P}$ = 14.9 Hz, 9H, P(C(C*H*$_3$)$_3$)$_2$), 0.42 (s, 9H, Si(C*H*$_3$)$_3$). ^{13}C{^{1}H} NMR (150.90 MHz, CD_2Cl_2): 354.9 (bs, Ru=CH), 175.4 (d, $^2J_{C,P}$ = 9.4 Hz, NCN), 121.2 (s, N(CH)$_2$N), 119.5 (d, $^3J_{C,P}$ = 8.6 Hz, N(CH)$_2$N), 59.6 (s, NC(CH$_3$)$_3$), 44.8 (d, $^1J_{C,P}$ = 28.2 Hz, PCH$_2$), 38.5 (d, $^1J_{C,P}$ = 21.3 Hz, P(C(CH$_3$)$_3$)$_2$), 34.6 (d, $^1J_{C,P}$ = 24.5 Hz, P(C(CH$_3$)$_3$)$_2$), 32.7 (s, NC(CH$_3$)$_3$), 29.3 (d, $^2J_{C,P}$ = 3.2 Hz, P(C(CH$_3$)$_3$)$_2$), 28.6 (d, $^2J_{C,P}$ = 2.3 Hz, P(C(CH$_3$)$_3$)$_2$), −0.9 (s, Si(CH$_3$)$_3$). ^{31}P{^{1}H} NMR (242.94 MHz, CD_2Cl_2): 124.6 (s). IR (KBr), ν (cm^{-1}): 3101 (w), 2951 (s), 2900 (s), 1936 (w), 1477 (s), 1370 (m), 1199 (m), 842 (s). MS (FAB$^+$), *m*/*z* (%): 540.1 [M]$^+$ (9), 505.2 [M − Cl]$^+$ (100), 454.1 [RuCl$_2$(NHCP)]$^+$ (15). HRMS (ESI$^+$), *m*/*z*: calcd for $C_{20}H_{41}Cl_2N_2PRuSi$ 540.1197; found 540.1166.

[RuCl$_2$($^{\mathrm{Mes}}$NHCP$^{t\mathrm{Bu}}$)(PMe$_3$)] (8). In a Schlenk tube complex **6** (60.0 mg, 65.8 μmol) was suspended in dichloromethane (6 mL), and a solution of PMe$_3$ in THF (125 μL, 125 μmol, 1 M) was added. The reaction mixture was stirred at room temperature for 1.5 h, resulting in the formation of a green solution. After filtration pentane (5 mL) was added to precipitate the product. The mother liquor was removed, and the solid was washed again with pentane (5 mL). The residue was dried under vacuum, affording a green solid in a 68% (45 mg) yield. ^{1}H NMR (300.13 MHz, CD_2Cl_2): 7.36 (m, 1H, N(C*H*)$_2$N), 7.27 (m, 1H, N(C*H*)$_2$N), 4.12 (d, $^2J_{H,P}$ = 6.4 Hz, 2H, PC*H*$_2$), 1.65 (d, $^2J_{H,P}$ = 7.0 Hz, 9H, P(C*H*$_3$)$_3$), 1.52 (s, 9H, NC(C*H*$_3$)$_3$), 1.16 (d, $^3J_{H,P}$ = 12.9 Hz, 18H, P(C(C*H*$_3$)$_3$)$_2$). ^{13}C{^{1}H} NMR (75.48 MHz, CD_2Cl_2): 191.4 (s, NCN), 119.5 (s, N(CH)$_2$N), 119.4 (s, N(CH)$_2$N), 59.1 (s, NC(CH$_3$)$_3$), 47.9 (d, $^1J_{C,P}$ = 25.1 Hz, PCH$_2$), 39.2 (d, $^1J_{C,P}$ = 20.4 Hz, P(C(CH$_3$)$_3$)$_2$), 32.1 (s, NC(CH$_3$)$_3$), 30.1 (d, $^2J_{C,P}$ = 2.4 Hz, P(C(CH$_3$)$_3$)$_2$), 15.0 (d, $^1J_{C,P}$ = 21.5 Hz, P(CH$_3$)$_3$). ^{31}P{^{1}H} NMR: (121.50 MHz, CD_2Cl_2): −5.5 (d, $^2J_{P,P}$ = 17.8 Hz), 120.7 (d, $^2J_{P,P}$ = 17.8 Hz). IR (KBr), ν (cm^{-1}): 3125 (w), 2963 (m), 2908 (m), 1393 (s), 1276 (s), 952 (s), 727 (m). MS (FAB$^+$), *m*/*z* (%): 530.2 [M]$^+$ (75), 495.2 [M − Cl]$^+$ (80), 454.1 [RuCl$_2$(NHCP)]$^+$ (100), 383.1 [Ru(NHCP)]$^+$ (30). HRMS (FAB$^+$), *m*/*z*: calcd for $C_{19}H_{40}Cl_2N_2P_2Ru$ 530.1087; found 530.1116. Anal. Calcd for $C_{19}H_{40}Cl_2N_2P_2Ru$: C, 43.02; H, 7.60; N, 5.28; P, 11.68. Found: C, 43.06; H, 7.60; N, 5.36; P, 11.38.

[RuCl$_2$($^{\mathrm{Mes}}$NHCP$^{t\mathrm{Bu}}$)(PPh$_3$)] (9a,b). In a Schlenk tube complex **6** (50.0 mg, 54.8 μmol) and PPh$_3$ (27.0 mg, 100 μmol, 2 equiv) were dissolved in dichloromethane (6 mL). The reaction mixture was stirred for 1.5 h at room temperature, resulting in a color change to a red solution. After filtration of the solution pentane (5 mL) was added to precipitate the product. The mother liquor was decanted, and the solid was washed with hexane (3 × 5 mL). The residue was dried under vacuum, affording a red solid in 67% (48 mg) yield. ^{1}H NMR (300.13 MHz, CD_2Cl_2), first set of signals: 7.13−7.44 (m, 15H, Ar), 6.98 (d, $^3J_{H,H}$ = 2.2 Hz, 1H, N(C*H*)$_2$N), 6.57 (d, $^3J_{H,H}$ = 2.0 Hz, 1H, N(C*H*)$_2$N), 3.27−3.40 (m, 1H, PC*H*$_2$), 2.45−2.54 (m, 1H, PC*H*$_2$), 1.37 (s, 9H, NC(C*H*$_3$)$_3$), 1.36 (d, $^3J_{H,P}$ = 14.2 Hz, 9H, PC(C*H*$_3$)$_3$), 1.20 (d, $^3J_{H,P}$ = 13.3 Hz, 9H, P(C(C*H*$_3$)$_3$)$_2$); second set of signals: 7.79−7.93 (m, 6H, Ar), 7.33 (m, 1H, N(C*H*)$_2$N), 7.24 (m, 1H, N(C*H*)$_2$N), 7.13−7.44 (m, 12H, Ar-*H*), 4.09 (d, $^2J_{H,P}$ = 6.4 Hz, 2H, PC*H*$_2$), 1.41 (s, 9H, NC(C*H*$_3$)$_3$), 1.07 (d, $^3J_{H,P}$ = 13.3 Hz, 18H, P(C(C*H*$_3$)$_3$)$_2$). The sample contains free PPh$_3$. ^{13}C{^{1}H} NMR (75.47 MHz, CD_2Cl_2), first set of signals: 183.1 (s, NCN), 129.5 (m, Ar), 129.0 (d, $^2J_{C,P}$ = 6.8 Hz, Ar), 128.3−128.8 (m, Ar), 121.0 (s, N(CH)$_2$N), 120.1 (d, $^3J_{C,P}$ = 7.1 Hz, N(CH)$_2$N), 59.8 (s, NC(CH$_3$)$_3$), 45.4 (d, $^1J_{C,P}$ = 24.8 Hz, PCH$_2$), 39.5 (d, $^1J_{C,P}$ = 19.3 Hz, P(C(CH$_3$)$_3$)$_2$), 36.4 (d, $^1J_{C,P}$ = 21.6 Hz, P(C(CH$_3$)$_3$)$_2$), 32.2 (s, NC(CH$_3$)$_3$), 31.8 (bs, P(C(CH$_3$)$_3$)$_2$), 29.7 (d, $^2J_{C,P}$ = 2.9 Hz, P(C(CH$_3$)$_3$)$_2$); second set of signals: 192.2 (s, NCN), 135.8 (d, $^2J_{C,P}$ = 10.3 Hz, Ar), 129.6 (d, $^3J_{C,P}$ = 1.3 Hz, Ar), 129.3 (s, Ar), 128.3−128.8 (m, Ar), 119.8 (d, $^4J_{C,P}$ = 3.9 Hz, N(CH)$_2$N), 119.3 (dd, $^3J_{C,P}$ = 7.6 Hz, $^4J_{C,P}$ = 2.1 Hz, N(CH)$_2$N), 58.8 (s, NC(CH$_3$)$_3$), 47.9 (d, $^1J_{C,P}$ = 29.9 Hz, CH$_2$), 39.8 (d, $^1J_{C,P}$ = 18.7 Hz, P(C(CH$_3$)$_3$)$_2$), 32.8 (s, NC(CH$_3$)$_3$), 30.3 (d, $^2J_{C,P}$ = 2.6 Hz, P(C(CH$_3$)$_3$)$_2$). (The sample contains free PPh$_3$.) ^{31}P{^{1}H} NMR (121.49 MHz, CD_2Cl_2, 223 K), first set of signals: 34.1 (d, $^2J_{P,P}$ = 32.3 Hz, PPh$_3$), 126.0 (d, $^2J_{P,P}$ = 32.3 Hz, P(C(CH$_3$)$_3$)$_2$); second set of signals: 24.5 (d, $^2J_{P,P}$ = 10.0 Hz, PPh$_3$), 108.3 (d, $^2J_{P,P}$ = 10.0 Hz, P(C(CH$_3$)$_3$)$_2$). (The sample contains free PPh$_3$ in a 2:1 ratio.) IR (KBr), ν (cm^{-1}): 3053 (w), 2960 (m), 2908 (m), 1480 (m), 1434 (s), 1366 (m), 744 (m), 697 (s), 527 (m). MS (FAB$^+$), *m*/*z* (%): 716.2 [M]$^+$ (5), 681.2 [M − Cl]$^+$ (55), 454.1 [Ru(NHCP)(Cl)$_2$]$^+$ (50), 383.1 [Ru(NHCP)]$^+$ (48), 262.1 [PPh$_3$]$^+$ (100). HRMS (FAB$^+$), *m*/*z*: calcd for $C_{34}H_{46}Cl_2N_2P_2Ru$ 716.1557; found 716.1650. Anal. Calcd for $C_{34}H_{46}Cl_2N_2P_2Ru$: C, 56.98; H, 6.47; N, 3.91; P, 8.64. Found: C, 56.93; H, 6.85; N, 3.95; P, 8.02.

[RuCl$_2$($^{\mathrm{Mes}}$NHCP$^{t\mathrm{Bu}}$)(PCy$_3$)] (10a,b). In a Schlenk tube complex **6** (30.2 mg, 33 μmol) and PCy$_3$ (5.2 mg, 66 μmol, 2 equiv) were dissolved in dichloromethane (6 mL). The reaction mixture was stirred at room temperature for 2 h, resulting in a color change to a red solution, which was filtered and concentrated under vacuum to ca. 0.5 mL. Diethyl ether (1 mL) was added, resulting in the product precipitation. The mother liquor was decanted, and the solid was washed again with diethyl ether (2 mL). The residue was dried under vacuum, affording a red solid in 87% (42 mg) yield. Mp: 127 °C (dec). ^{31}P{^{1}H} NMR (202.46 MHz, CD_2Cl_2): 33.4 (s, PCy$_3$), 39.6 (s, PCy$_3$), 94.0 (s, P(C(CH$_3$)$_3$)$_2$), 116.0 (s, P(C(CH$_3$)$_3$)$_2$). The two species are

dx.doi.org/10.1021/om300487r | *Organometallics* 2013, 32, 29−46

in a 1:1 ratio. IR (KBr), ν (cm^{-1}): 2933 (w), 2857 (m), 1447 (m), 1371 (m), 1238 (w), 1098 (s), 806 (m). MS (FAB^+), m/z (%): 699.5 $[M]^+$ (30), 454.1 $[Ru(NHCP)(Cl)_2]^+$ (80), 383.1 $[Ru(NHCP)]^+$ (90). Anal. Calcd for $C_{34}H_{64}Cl_2N_2P_2Ru$: C, 55.57; H, 8.78; N, 3.81. Found: C, 54.57; H, 8.57; N, 1.71.

[$RuCl_2$(^{Mes}NHCP^{tBu})(py_2)] (11). In a Schlenk tube complex **6** (10.3 mg, 11 μmol) and pyridine (3.0 mg, 38 μmol, 3.6 equiv) were dissolved in CD_2Cl_2 (0.5 mL), affording a green solution, which upon cooling to −30 °C became brown. Crystals suitable for X-ray analysis were obtained by slow evaporation of a concentrated solution of complex **6** in pyridine. ^{1}H NMR (300.13 MHz, pyridine-d_5): 7.53 (d, $^3J_{H,H}$ = 2.1 Hz, 1H, N(C*H*)$_2$N), 7.39 (d, $^3J_{H,H}$ = 2.1 Hz, 1H, N(C*H*)$_2$N), 4.76 (d, $^2J_{H,P}$ = 4.7 Hz, 2H, PCH_2), 1.49 (s, 9H, NC(CH_3)$_3$), 1.33 (d, $^3J_{H,P}$ = 11.3 Hz, 18H, P(C(CH_3)$_3$)$_2$), signals of the coordinated pyridines were not detected because of exchange with the solvent. ^{13}C{^{1}H} NMR (75.47 MHz, pyridine-d_5): 192.2 (d, $^2J_{C,P}$ = 9.9 Hz, NCN), 129.8 (s, py), 129.0 (s, py), 122.4 (s, N(CH)$_2$N), 120.9 (d, $^3J_{C,P}$ = 5.5 Hz, N(CH)$_2$N), 60.4 (s, NC(CH$_3$)$_3$), 48.6 (d, $^1J_{C,P}$ = 23.6 Hz, PCH$_2$), 37.6 (d, $^1J_{C,P}$ = 11.5 Hz, P(C(CH$_3$)$_3$)$_2$), 32.4 (s, NC(CH$_3$)$_3$), 31.0 (d, $^2J_{C,P}$ = 2.7 Hz, P(C(CH$_3$)$_3$)$_2$), signals of the coordinated pyridines were not detected because of exchange with the solvent. ^{31}P{^{1}H} NMR (121.50 MHz, pyridine-d_5): 84.9 (s). Partial NMR data in CD_2Cl_2: ^{1}H NMR (500.13 MHz, CD_2Cl_2, 193 K): 9.36 (bs, 1H, py), 9.05 (bs, 1H, py), 8.44 (bs, 1H, py), 8.06 (bs, 1H, py), 7.65 (d, $^3J_{H,H}$ = 4.7 Hz, 2H, py), 7.19−7.32 (m, 3H, py), 7.15 (bs, 1H, py) 7.03 (bs, 1H, N(C*H*)$_2$N), 6.95 (bs, 1H, N(C*H*)$_2$N), 4.62 (d, $^2J_{H,P}$ = 11.5 Hz, 1H, PCH_2), 4.07−4.17 (m, 1H, PCH_2), 1.57 (d, $^3J_{H,P}$ = 13.1 Hz, 3H, P(C(CH_3)$_3$)$_2$), 1.31 (bs, 3H, P(C(CH_3)$_3$)$_2$), 1.22 (bs, 9H, NC(CH_3)$_3$), 0.98 (d, $^3J_{H,P}$ = 8.8 Hz, 9H, P(C(CH_3)$_3$)$_2$), 0.44 (d, $^3J_{H,P}$ = 9.8 Hz, 3H, P(C(CH_3)$_3$)$_2$). ^{31}P{^{1}H} NMR (200.46 MHz, CD_2Cl_2, 193 K): 80.5 (s). MS (FAB^+), m/z (%): 622.4 $[M]^+$ (10), 587.4 $[M - Cl]^+$ (7), 538.4 $[M - py]^+$ (40).

[$RuCl_2$(^{Mes}NHCP^{tBu})(py)] (12). In a Schlenk tube complex **6** (60.0 mg, 66 μmol) and a solution of pyridine in THF (260 mL, 13 μmol, 0.5 M, 1 equiv) were dissolved in THF (5 mL). The green solution was heated for 1 h at 50 °C and then filtered and concentrated under vacuum to ca. 0.5 mL. Pentane (8 mL) was added, resulting in the product precipitation. The residue was then washed with pentane (3 × 8 mL) and dried under vacuum, affording a green solid in 68% (47 mg) yield. ^{1}H NMR (500.13 MHz, CD_2Cl_2): 9.60 (dd, $^3J_{H,H}$ = 6.4 Hz, $^4J_{H,H}$ = 1.4 Hz, 2H, Py), 7.87 (t, $^3J_{H,H}$ = 7.6 Hz, 1H, Py), 7.41−7.46 (m, 2H, Py), 7.28 (d, $^3J_{H,H}$ = 2.2 Hz, 1H, N(C*H*)$_2$N), 7.22 (d, $^3J_{H,H}$ = 2.2 Hz, 1H, N(C*H*)$_2$N), 4.02 (d, $^2J_{H,P}$ = 6.4 Hz, 2H, PCH_2), 1.67 (s, 9H, NC(CH_3)$_3$), 1.15 (d, $^3J_{H,P}$ = 13.1 Hz, 18H, P(C(CH_3)$_3$)$_2$). ^{13}C{^{1}H} NMR (125.76 MHz, CD_2Cl_2): 194.7 (d, $^2J_{C,P}$ = 12.5 Hz, NCN), 155.1 (s, Py), 137.1 (s, Py), 124.4 (s, Py), 119.2 (d, $^3J_{C,P}$ = 7.7 Hz, N(CH)$_2$N), 119.1 (s, N(CH)$_2$N), 58.8 (s, NC(CH$_3$)$_3$), 47.4 (d, $^1J_{C,P}$ = 26.9 Hz, PCH$_2$), 38.9 (d, $^1J_{C,P}$ = 20.2 Hz, P(C(CH$_3$)$_3$)$_2$), 32.2 (s, NC(CH$_3$)$_3$), 30.3 (d, $^2J_{C,P}$ = 2.9 Hz, P(C(CH$_3$)$_3$)$_2$). ^{31}P{^{1}H} NMR (202.46 MHz, CD_2Cl_2): 122.4 (s). ^{15}N{^{1}H} NMR (50.70 MHz, CD_2Cl_2): −190.0 (Im-*N*3), −167.2 (Im-*N*1), −107.5 (coordinated pyridine), −64.7 (contains noncoordinated pyridine). IR (KBr), ν (cm^{-1}): 2962 (m), 2899 (w), 1598 (w), 1482 (m), 1443 (s), 1368 (s), 1235 (s), 699 (s). MS (FAB^+), m/z (%): 533.2 $[M]^+$ (40), 454.1 $[Ru(NHCP)(Cl)_2]^+$ (100). HRMS (FAB^+), m/z: calcd for $C_{21}H_{36}Cl_2N_3PRu$: 533.1067. Found: 533.1093. Anal. Calcd for $C_{21}H_{36}Cl_2N_3PRu$: C, 47.28; H, 6.80; N, 7.88. Found: C, 47.97; H, 6.93; N, 7.73.

[$RuCl_2$(^{Mes}NHCP^{tBu})(bipy)] (13). In a Schlenk tube complex **6** (30.0 mg, 32.9 μmol) was dissolved in CH_2Cl_2 (5 mL), and 2,2′-bipyridine (10.8 mg, 69.2 μmol) was added. The reaction mixture was stirred at 40 °C for 20 h, affording a deep red solution. The solvent was removed under vacuum, and the residue was washed with pentane (4 × 10 mL) and then dried under vacuum, affording the product in 87% (35 mg) yield. ^{1}H NMR (250.10 MHz, $CDCl_3$): 9.65 (d, $^3J_{H,H}$ = 5.1 Hz, 1H, bipy), 8.79 (d, $^2J_{H,H}$ = 8.4 Hz, 1H, bipy), 8.69 (d, $^3J_{H,H}$ = 8.4 Hz, 1H, bipy), 8.20 (t, $^3J_{H,H}$ = 8.4 Hz, 1H, bipy), 7.88 (t, $^3J_{H,H}$ = 8.4 Hz, 1H, bipy), 7.76 (d, $^3J_{H,H}$ = 1.8 Hz, 1H, N(C*H*)$_2$N), 7.68 (t, $^3J_{H,H}$ = 6.5 Hz, 1H, bipy), 7.45 (d, $^3J_{H,H}$ = 6.0 Hz, 1H, bipy), 7.35 (t, $^3J_{H,H}$ = 6.5 Hz, 1H, bipy), 7.28 (d, $^3J_{H,H}$ = 1.8 Hz, 1H, N(C*H*)$_2$N), 4.48 (d, $^2J_{H,P}$ = 14.0 Hz, 1H, PCH_2), 4.28 (dd, $^2J_{H,P}$ = 10.5 Hz, 1H, PCH_2), 1.25 (s, 9H, NC(CH_3)$_3$), 0.54 (d, $^3J_{H,P}$ = 13.8 Hz, 18H, P(C(CH_3)$_3$)$_2$). ^{31}P{^{1}H} NMR (101.20 MHz, $CDCl_3$): 119.4 (s). MS (FAB^+), m/z (%): 575.2 $[M - Cl]^+$ (95). Anal. Calcd for $C_{26}H_{40}Cl_2N_4PRu$: C, 51.06; H, 6.59; N, 9.16. Found: C, 50.90; H, 6,51; N, 9.01.

3-*tert*-Butyl-1-(di-*tert*-butylphosphinomethyl)imidazolium Iodide (14). To a suspension of **4a** (50.0 mg, 161 μmol) in acetone (5 mL) was added NaI (23.5 mg, 157 μmol) as a solid, and the reaction mixture was stirred for 16 h at room temperature. The reaction mixture was filtered through Celite, and the solvent removed *in vacuo*. The product was dried under vacuum, affording a white solid in 99% (64 mg) yield. ^{1}H NMR (300.08 MHz, CD_2Cl_2): 10.44 (s, 1H, NC*H*N), 7.67 (s, 1H, N(C*H*)$_2$N), 7.41 (t, $^3J_{H,H}$ = 1.9 Hz, 1H, N(C*H*)$_2$N), 4.78 (bs, 2H, CH_2P), 1.70 (s, 9H, NC(CH_3)$_3$), 1.21 (d, $^3J_{H,P}$ = 11.8 Hz, 18H, PC(CH_3)$_3$). ^{13}C{^{1}H} NMR (75.46 MHz, CD_2Cl_2): 136.1 (d, $^3J_{C,P}$ = 5.2 Hz, NCHN), 123.1 (d, $^3J_{C,P}$ = 10.3 Hz, N(CH)$_2$N), 119.4 (s, N(CH)$_2$N), 45.5 (d, $^1J_{C,P}$ = 26.4 Hz, CH$_2$P), 32.7 (d, $^1J_{C,P}$ = 19.0 Hz, PC(CH$_3$)$_3$), 30.5 (s, PC(CH$_3$)$_3$), 29.8 (d, $^1J_{C,P}$ = 13.2 Hz, PC(CH$_3$)$_3$), 26.4 (s, PC(CH$_3$)$_3$). ^{31}P{^{1}H} NMR (121.47 MHz, CD_2Cl_2): 29.1 (s). MS (ESI), m/z (%): 283.23 $[M]^+$ (100). Anal. Calcd for $C_{16}H_{32}IN_2P$: C, 46.83; H, 7.86; N, 6.83. Found: C, 45.16; H, 7.65; N, 6.62.

[AgI(^{tBu}NHCP^{tBu})]$_2$ (15). Into a Schlenk tube under argon were added ligand **8** (200 mg, 487 μmol) and Ag_2O (56.5 mg, 244 μmol) as solids, and then CH_2Cl_2 (5 mL) was added. The reaction mixture was heated at 50 °C under stirring for 2 h, resulting in a light yellow solution. The solution was filtered through Celite. The filtrate was dried under vacuum, affording a light brown solid in 89% (174 mg) yield. ^{1}H NMR (300.19 MHz, CD_2Cl_2): 7.39 (s, 1H, N(C*H*)$_2$N), 7.25 (t, $^3J_{H,H}$ = 1.9 Hz, 1H, N(C*H*)$_2$N), 4.42 (s, 2H, CH_2P), 1.70 (s, 9H, NC(CH_3)$_3$) 1.23 (d, $^3J_{H,P}$ = 12.4 Hz, 18H, PC(CH_3)$_3$). ^{13}C{^{1}H} NMR (75.48 MHz, CD_2Cl_2): 186.1 (bs, NCN), 121.8 (s, N(CH)$_2$N), 119.3 (d, $J_{C,P}$ = 4.0 Hz, N(CH)$_2$N), 46.7 (d, $^1J_{C,P}$ = 4.6 Hz, CH$_2$P), 33.6 (d, $^1J_{C,P}$ =12.1 Hz, PC(CH$_3$)$_3$), 31.9 (s, NC(CH$_3$)$_3$), 30.0 (d, $^2J_{C,P}$ =10.9 Hz, PC(CH$_3$)$_3$), 27.0 (s, NC(CH$_3$)$_3$). ^{31}P{^{1}H} NMR (121.47 MHz, CD_2Cl_2): 30.44 (bs). HRMS (FAB^+), m/z (%): calcd for $C_{16}H_{31}AgN_2P$: 389.1276 (100); found 389.1278 (93). Anal. Calcd for $C_{16}H_{31}AgIN_2P$: C, 37.16; H, 6.04; N, 5.42. Found: C, 35.52; H, 5.76; N, 5.12.

[$RuCl_2$(^{Mes}NHCP^{tBu})(benzylidene)] (17). First-generation Grubbs catalyst (47.8 mg, 58 μmol) was dissolved in toluene (1 mL), and to it was added **5b** (20.0 mg, 58 μmol) in toluene (1 mL). The reaction mixture was stirred for 16 h at room temperature, resulting in a color change to brownish-green and the formation of a green solid. The slurry was filtered through a short plug of Celite, and the solid on the plug was washed with toluene (2 × 2 mL). The solid was eluted with THF (3 mL), dried under vacuum, and then redissolved in THF (1 mL). The solution was passed through a silica gel plug and washed out with another 3 mL of THF, leaving a brown material on the plug. The green solution was dried under vacuum, affording a green solid in 29% (10 mg) yield of an unclean product. Partial spectral data: ^{1}H NMR (200.15 MHz, acetone-d_6): 14.97 (d, $^3J_{H,P}$ = 12.5 Hz, 1H, Ru=C*H*), 8.42 (d, J = 7.8 Hz, 2H, Ar), 7.96 (d, J = 2.0 Hz, 1H, N(C*H*)$_2$N), 7.59 (t, J = 7.6 Hz, 1H, Ar), 7.32 (d, J = 7.3 Hz, 2H, Ar), 6.91 (dd, J = 2.1, 0.6 Hz, 1H, N(C*H*)$_2$N), 6.75 (bs, 1H, Mes), 6.51 (bs, 1H, Mes), 5.19 (dd, J = 14.7, 10.8 Hz, 1H, PCH_2), 4.91 (dd, J = 14.7, 1.7 Hz, 1H, PCH_2), 4.29 (t, J = 7.0 Hz, 1H), 2.17 (s, 3H, Mes-CH_3), 1.98 (s, 3H, Mes-CH_3), 1.47 (d, J = 12.7 Hz, 9H, PC(CH_3)$_3$), 1.19 (d, J = 14.4 Hz, 9H, PC(CH_3)$_3$), 1.16 (s, 3H, Mes-CH_3). ^{31}P NMR (81.02 MHz, acetone-d_6): 107.2 (s).

[$RuCl_2$(^{tBu}NHCP^{tBu})(3-phenyl-1*H*-inden-1-ylidene)] (18). In a Schlenk tube ligand **5b** (20.0 mg, 58.1 μmol) and Umicore M1 catalyst (53.6 mg, 58.1 μmol) were dissolved in toluene (4 mL). The reaction mixture was heated at 80 °C for 10 h, resulting in a color change from reddish-brown to red and in the formation of a red solid. The slurry was filtered through cotton and a Celite plug. The solid on the plug was washed with toluene (4 mL) and then dissolved partially with THF (2 mL) and completely dissolved with dichloromethane (5 mL). The combined solutions were dried under vacuum, affording a red

dx.doi.org/10.1021/om300487r | *Organometallics* 2013, 32, 29−46

solid in 60% (25 mg) yield. ^{1}H NMR (600.13 MHz, CD_2Cl_2): 8.94 (d, $J_{H,P}$ = 6.9 Hz, 1H, Ind-C*H*), 7.66 (s, 1H, N(C*H*)$_2$N), 7.58 (d, $^3J_{H,H}$ = 7.4 Hz, 2H, Ind-Ar), 7.51 (t, $^3J_{H,H}$ = 7.5 Hz, 1H, Ind-Ar), 7.41 (m, 3H, Ind-Ar), 7.24 (t, $^3J_{H,H}$ = 7.4 Hz, 1H, Ind-Ar), 7.16 (m, 2H, Ind-Ar), 6.81 (s, 1H, Mes-C*H*), 6.76 (s, 1H, N(C*H*)$_2$N), 6.62 (s, 1H, Mes-C*H*), 4.90 (dd, $^2J_{H,P}$ = 14.4 Hz, $^2J_{H,H}$ = 10.6 Hz, 1H, PCH_2), 4.45 (d, $^2J_{H,P}$ = 14.4 Hz, 1H, PCH_2), 2.23 (s, 3H, Mes-*o*-CH_3), 1.88 (s, 3H, Mes-*o*-CH_3),1.47 (d, $^3J_{H,P}$ = 13.0 Hz, 9H, P(C(CH_3)$_3$), 1.41 (s, 3H, Mes-*p*-CH_3), 1.14 (d, $^3J_{H,P}$ = 14.7 Hz, 9H, P(C(CH_3)$_3$). ^{13}C{^{1}H} NMR (150.90 MHz, CD_2Cl_2): 284.4 (d, $^2J_{C,P}$ = 12.1 Hz, Ru=*C*H), 181.2 (d, $^2J_{C,P}$ = 9.1 Hz, NCN), 148.7 (s, Ind), 140.5 (s, Ind), 138.79 (s, Ind), 137.3 (d, $^3J_{C,P}$ = 6.0 Hz, Ind), 137.1 (s, Ind), 136.3 (d, $^4J_{C,P}$ = 1.5 Hz, Ind), 130.7 (s, Ind), 130.3 (d, $^3J_{C,P}$ = 7.5 Hz, Ind), 129.6 (s, Ind), 129.5 (d, $^4J_{C,P}$ = 1.5 Hz, Ind), 128.8 (s, Ind), 128.7 (d, $^4J_{C,P}$ = 3.0 Hz, Ind), 126.8 (s, Ind), 126.5 (s, Ind), 121.1 (d, $^3J_{C,P}$ = 7.5 Hz, N(*C*H)$_2$N), 118.3 (s, N(*C*H)$_2$N), 45.3 (d, $^1J_{C,P}$ = 9.0 Hz, P*C*H$_2$), 38.1 (d, $^1J_{C,P}$ = 18.1 Hz, P(*C*(CH$_3$)$_3$), 36.6 (d, $^1J_{C,P}$ = 18.1 Hz, P(*C*(CH$_3$)$_3$), 30.7 (d, $^2J_{C,P}$ = 3.0 Hz, P(C(*C*H$_3$)$_3$), 29.5 (d, $^2J_{C,P}$ = 3.0 Hz, P(C(*C*H$_3$)$_3$), 21.3 (s, Mes-*C*H$_3$), 18.8 (s, Mes-*C*H$_3$), 17.9 (s, Mes-*C*H$_3$). ^{31}P{^{1}H} NMR (242.94 MHz, CD_2Cl_2): 102.4 (s). HRMS (FAB$^+$), *m*/*z*: calcd for $C_{36}H_{43}ClN_2PRu$: 671.1903; found 671.1887. Anal. Calcd for $C_{36}H_{43}Cl_2N_2PRu$: C, 61.18; H, 6.13; N, 3.96. Found: C, 59.12; H, 6.57; N, 3.75.

X-ray Diffraction Studies. For the X-ray diffraction studies data sets were collected on Bruker CCD diffractometers ("Smart CCD" for **3b**, **5a**, **6**, **7b**, **7e**, **7f**, **8**, **12** and "APEX" for **4a**, **7a**, **7c**, **9b**, **13**, **16a**, **16b** with Mo Kα radiation (λ = 0.71073 Å) at 200 K (100 K for **4a**, **13**)). A complete sphere in reciprocal space was covered by 0.3 deg ω-scans in all cases. For all data sets the intensities were corrected for Lorentz and polarization effects, and an empirical absorption correction, based on the Laue symmetry of the reciprocal space, was applied using SADABS (2008/1).[31] All structures were solved by direct methods and refined against F^2 with a full-matrix least-squares algorithm using the SHELXTL (Version 2008/4) software package.[32] If not noted differently below hydrogen atoms were treated using appropriate riding models. CCDC 643287 (**2**), 643288 (**3a**), 887432 (**3b**), 643289 (**4a**), 643291 (**5a**), 887433 (**6**), 887434 (**7a**), 887435 (**7b**), 887436 (**7c**), 887437 (**7e**), 887438 (**7f**), 887439 (**8**), 887440 (**9b**), 887441 (**12**), 887442 (**13**), 887443 (**16a**), and 887444 (**16b**) contain the supplementary crystallographic data for this paper. These data can be obtained free of charge from The Cambridge Crystallographic Data Centre via www.ccdc.cam.ac.uk/data_request/cif.

3b. Colorless crystals (polyhedron), 0.17 × 0.11 × 0.05 mm^3, triclinic, $P\bar{1}$, Z = 2, a = 8.5358(2) Å, b = 13.0227(3) Å, c = 15.8524(4) Å, α = 101.698(1)°, β = 98.601(1)°, γ = 91.077(1)°, V = 1703.94(7) Å^3, ρ = 1.271 g/cm^3, θ_{max} = 20.83°, 9487 reflections measured, 3568 unique (R_{int} = 0.0683), 2286 observed ($I > 2\sigma(I)$), μ = 0.41 mm^{-1}, T_{min} = 0.93, T_{max} = 0.98, 415 parameters refined, goodness of fit 1.03 for observed reflections, final residual values R1(F) = 0.068, wR(F^2) = 0.131 for observed reflections, residual electron density −0.35 to 0.47 e Å^{-3}.

4a. Colorless crystals (polyhedron), 0.21 × 0.18 × 0.17 mm^3, triclinic, $P\bar{1}$, Z = 2, a = 8.8210(10) Å, b = 11.2465(13) Å, c = 13.8864(16) Å, α = 79.030(2)°, β = 72.245(2)°, γ = 87.263(2)°, V = 1287.9(3) Å^3, ρ = 0.983 g/cm^3, T = 100(2) K, θ_{max} = 28.31°, 13 037 reflections measured, 6243 unique (R_{int} = 0.0232), 5400 observed ($I > 2\sigma(I)$), μ = 0.25 mm^{-1}, T_{min} = 0.95, T_{max} = 0.96, 294 parameters refined, the "carbene H" H1 was refined isotropically, goodness of fit 1.11 for observed reflections, final residual values R1(F) = 0.066, wR(F^2) = 0.181 for observed reflections, residual electron density −0.30 to 0.60 e Å^{-3}.

5a. Colorless crystals (polyhedron), 0.38 × 0.2 × 0.2 mm^3, monoclinic, $P2_1/c$, Z = 4, a = 12.4480(1) Å, b = 14.2069(3) Å, c = 11.5696(2) Å, α = 90°, β = 116.6650(10)°, γ = 90°, V = 1828.45(5) Å^3, ρ = 1.026 g/cm^3, θ_{max} = 25.35°, 15 701 reflections measured, 3332 unique (R_{int} = 0.0621), 2334 observed ($I > 2\sigma(I)$), μ = 0.14 mm^{-1}, 189 parameters refined, the hydrogen atoms H3 and H4 at the NHC ring were refined isotropically, goodness of fit 1.02 for observed reflections, final residual values R1(F) = 0.042, wR(F^2) = 0.082 for observed reflections, residual electron density −0.23 to 0.16 e Å^{-3}.

6. Brown crystals (polyhedron), 0.30 × 0.19 × 0.17 mm^3, monoclinic, $P2_1/n$, Z = 2, a = 11.8023(1) Å, b = 18.0801(1) Å, c = 12.1946(1) Å, α = 90°, β = 116.5820(10)°, γ = 90°, V = 2327.10(3) Å^3, ρ = 1.539 g/cm^3, θ_{max} = 27.42°, 22 349 reflections measured, 5300 unique (R_{int} = 0.0315), 4831 observed ($I > 2\sigma(I)$), μ = 1.21 mm^{-1}, T_{min} = 0.71, T_{max} = 0.82, 246 parameters refined, goodness of fit 1.06 for observed reflections, final residual values R1(F) = 0.023, wR(F^2) = 0.056 for observed reflections, residual electron density −0.41 to 0.50 e Å^{-3}.

7a. Dark orange crystals (polyhedron), 0.18 × 0.09 × 0.08 mm^3, trigonal, space group $P3_121$, Z = 6, a = 12.4946(11) Å, b = 12.4946(11) Å, c = 31.855(4) Å, α = 90°, β = 90°, γ = 120°, V = 4306.8(7) Å^3, ρ = 1.456 g/cm^3, θ_{max} = 28.35°, 45 832 reflections measured, 7137 unique (R_{int} = 0.0615), 6633 observed ($I > 2\sigma(I)$), μ = 0.99 mm^{-1}, T_{min} = 0.84, T_{max} = 0.93, 289 parameters refined, Flack absolute structure parameter 0.07(3), goodness of fit 1.10 for observed reflections, final residual values R1(F) = 0.035, wR(F^2) = 0.072 for observed reflections, residual electron density −0.37 to 0.73 e Å^{-3}.

7b. Green crystals (polyhedron), 0.22 × 0.14 × 0.04 mm^3, monoclinic, $P2_1/n$, Z = 4, a = 9.6909(1) Å, b = 26.8891(1) Å, c = 12.5386(2) Å, α = 90°, β = 103.3680(10)°, γ = 90°, V = 3178.78(6) Å^3, ρ = 1.569 g/cm^3, θ_{max} = 24.71°, 24 728 reflections measured, 5424 unique (R_{int} = 0.0866), 3792 observed ($I > 2\sigma(I)$), μ = 2.24 mm^{-1}, T_{min} = 0.64, T_{max} = 0.92, 319 parameters refined, goodness of fit 1.08 for observed reflections, final residual values R1(F) = 0.063, wR(F^2) = 0.126 for observed reflections, residual electron density −1.27 to 1.37 e Å^{-3}.

7c. Green crystals (needles), 0.77 × 0.04 × 0.03 mm^3, monoclinic, $P2_1/n$, Z = 8, a = 9.5624(13) Å, b = 27.160(4) Å, c = 23.802(3) Å, α = 90°, β = 99.976(3)°, γ = 90°, V = 6088.1(15) Å^3, ρ = 1.441 g/cm^3, θ_{max} = 22.55°, 37 093 reflections measured, 7971 unique (R_{int} = 0.1432), 6469 observed ($I > 2\sigma(I)$), μ = 0.87 mm^{-1}, T_{min} = 0.55, T_{max} = 0.97, 636 parameters refined, goodness of fit 1.35 for observed reflections, final residual values R1(F) = 0.147, wR(F^2) = 0.255 for observed reflections, residual electron density −1.59 to 1.45 e Å^{-3}.

7e. Green crystals (polyhedron), 0.18 × 0.18 × 0.10 mm^3, monoclinic, $P2_1/n$, Z = 4, a = 10.0971(1) Å, b = 21.0977(2) Å, c = 11.9795(2) Å, α = 90°, β = 96.5740(10)°, γ = 90°, V = 2535.16(5) Å^3, ρ = 1.463 g/cm^3, θ_{max} = 27.49°, 25 082 reflections measured, 5794 unique (R_{int} = 0.0839), 4607 observed ($I > 2\sigma(I)$), μ = 0.91 mm^{-1}, 284 parameters refined, the "carbene H" H20 was refined isotropically, goodness of fit 1.05 for observed reflections, final residual values R1(F) = 0.035, wR(F^2) = 0.079 for observed reflections, residual electron density −0.57 to 0.60 e Å^{-3}.

7f. Colorless crystals (polyhedron), 0.26 × 0.24 × 0.14 mm^3, orthorhombic, $P2_12_12_1$, Z = 4, a = 10.9174(1) Å, b = 16.107 Å, c = 16.7379(1) Å, α = 90°, β = 90°, γ = 90°, V = 2943.38(3) Å^3, ρ = 1.412 g/cm^3, θ_{max} = 27.49°, 29 950 reflections measured, 6745 unique (R_{int} = 0.0475), 6272 observed ($I > 2\sigma(I)$), μ = 1.00 mm^{-1}, T_{min} = 0.78, T_{max} = 0.87, 315 parameters refined, hydrogen atom H20 at C20 was refined isotropically, Flack absolute structure parameter 0.03(2), goodness of fit 1.10 for observed reflections, final residual values R1(F) = 0.027, wR(F^2) = 0.060 for observed reflections, residual electron density −0.54 to 0.53 e Å^{-3}.

8. Green crystals (polyhedron), 0.42 × 0.24 × 0.10 mm^3, orthorhombic, $Pca2_1$, Z = 4, a = 13.1234(2) Å, b = 15.9143(2) Å, c = 12.1529(1) Å, α = 90°, β = 90°, γ = 90°, V = 2538.13(5) Å^3, ρ = 1.388 g/cm^3, θ_{max} = 27.47°, 25 223 reflections measured, 5794 unique (R_{int} = 0.0398), 5129 observed ($I > 2\sigma(I)$), μ = 0.96 mm^{-1}, T_{min} = 0.69, T_{max} = 0.91, 247 parameters refined, Flack absolute structure parameter 0.02(2), goodness of fit 1.05 for observed reflections, final residual values R1(F) = 0.026, wR(F^2) = 0.049 for observed reflections, residual electron density −0.41 to 0.34 e Å^{-3}.

9b. Violet crystals (plates), 0.23 × 0.15 × 0.01 mm^3, monoclinic, $P2_1/c$, Z = 4, a = 13.3716(8) Å, b = 14.0724(9) Å, c = 21.8737(14) Å, α = 90°, β = 99.899(2)°, γ = 90°, V = 4054.7(4) Å^3, ρ = 1.452 g/cm^3, θ_{max} = 28.36°, 41 839 reflections measured, 10 107 unique (R_{int} = 0.0892), 8446 observed ($I > 2\sigma(I)$), μ = 0.89 mm^{-1}, T_{min} = 0.82, T_{max} = 0.994 33 parameters refined, goodness of fit 1.36 for observed

reflections, final residual values R1(F) = 0.102, wR(F^2) = 0.150 for observed reflections, residual electron density −1.59 to 0.96 e Å^{-3}.

12. Orange crystals (polyhedron), 0.22 × 0.12 × 0.08 mm^3, monoclinic, $P2_1/n$, Z = 4, a = 18.1448(6) Å, b = 9.1268(3) Å, c = 19.6120(6) Å, α = 90°, β = 93.8720(10)°, γ = 90°, V = 3240.41(18) Å^3, ρ = 1.418 g/cm^3, θ_{max} = 27.49°, 32 713 reflections measured, 7426 unique (R_{int} = 0.1334), 5517 observed ($I > 2\sigma(I)$), μ = 0.73 mm^{-1}, T_{min} = 0.86, T_{max} = 0.943 71 parameters refined, goodness of fit 1.13 for observed reflections, final residual values R1(F) = 0.052, wR(F^2) = 0.105 for observed reflections, residual electron density −0.85 to 0.69 e Å^{-3}.

13. Black crystals (polyhedron), 0.28 × 0.23 × 0.17 mm^3, monoclinic, $P2_1/n$, Z = 4, a = 12.6218(14) Å, b = 16.0062(17) Å, c = 16.0036(17) Å, α = 90°, β = 99.837(2)°, γ = 90°, V = 3185.6(6) Å^3, ρ = 1.450 g/cm^3, T = 100(2) K, θ_{max} = 28.33°, 33 225 reflections measured, 7905 unique (R_{int} = 0.0261), 7151 observed ($I > 2\sigma(I)$), μ = 0.90 mm^{-1}, T_{min} = 0.79, T_{max} = 0.86, 400 parameters refined, goodness of fit 1.08 for observed reflections, final residual values R1(F) = 0.033, wR(F^2) = 0.076 for observed reflections, residual electron density −0.71 to 1.71 e Å^{-3}.

16a. Colorless crystals (polyhedron), 0.17 × 0.14 × 0.14 mm^3, triclinic, $P\bar{1}$, Z = 1, a = 9.7387(9) Å, b = 11.1342(10) Å, c = 13.2867(16) Å, α = 65.277(2)°, β = 77.942(2)°, γ = 85.113(2)°, V = 1279.8(2) Å^3, ρ = 1.599 g/cm^3, T = 200(2) K, θ_{max} = 28.3°, 13 678 reflections measured, 6314 unique (R_{int} = 0.0521), 5470 observed ($I > 2\sigma(I)$), μ = 2.07 mm^{-1}, T_{min} = 0.72, T_{max} = 0.76, 283 parameters refined, goodness of fit 1.03 for observed reflections, final residual values R1(F) = 0.027, wR(F^2) = 0.072 for observed reflections, residual electron density −1.20 to 1.00 e Å^{-3}.

16b. Colorless crystals (polyhedron), 0.18 × 0.09 × 0.04 mm^3, orthorhombic, $C222$, Z = 8, a = 18.139(4) Å, b = 21.706(4) Å, c = 24.619(5) Å, α = 90°, β = 90°, γ = 90°, V = 9694(4) Å^3, ρ = 1.60 g/cm^3, T = 200(2) K, θ_{max} = 25.8°, 42 272 reflections measured, 9282 unique (R_{int} = 0.0577), 6847 observed ($I > 2\sigma(I)$), μ = 2.184 mm^{-1}, T_{min} = −0.8, T_{max} = 25.8, 458 parameters refined, goodness of fit 1.08 for observed reflections, final residual values R1(F) = 0.058, wR(F^2) = 0.132 for observed reflections, residual electron density −0.76 to 0.74 e Å^{-3}.

■ ASSOCIATED CONTENT

Supporting Information

This material is available free of charge via the Internet at http://pubs.acs.org.

■ AUTHOR INFORMATION

Corresponding Author

*E-mail: ph@oci.uni-heidelberg.de.

Present Addresses

[§]Sandoz AG, Frankfurt, Germany.
[⊥]Freudenberg, Weinheim, Germany.
[∥]Faculdade de Ciências Integradas do Pontal, Brazil.

Notes

The authors declare no competing financial interest.

■ ACKNOWLEDGMENTS

H.S. and P.H. work at CaRLa (Catalysis Research Laboratory) of Heidelberg University, being cofinanced by the University of Heidelberg, the State of Baden-Wuerttemberg, and BASF SE. We gratefully acknowledge generous support from these institutions. Dr. Rommy Haufe has contributed valuable advice for NHCP ligand synthesis, worked out in the context of her studies of NHCP complexes of the nickel triad.[33] A.L.B. thanks DAAD, FAPESP, CNPq, CAPES, and FAPEMIG for financial support and fellowships.

■ DEDICATION

Dedicated to Prof. Roald Hoffmann on the occasion of his 75th birthday.

■ REFERENCES

(1) For recent reviews, see: (a) Vougioukalakis, G. C.; Grubbs, R. H. *Chem. Rev.* **2010**, *110*, 1746. (b) Lozano-Vila, A. M.; Monsaert, S.; Bajek, A.; Verpoort, F. *Chem. Rev.* **2010**, *110*, 4865. (c) Samojłowicz, C.; Bieniek, M.; Grela, K. *Chem. Rev.* **2009**, *109*, 3708. (d) Diesendruck, C. E.; Tzur, E.; Lemcoff, N. G. *Eur. J. Inorg. Chem.* **2009**, 4185.

(2) For hydroxyalkyl-NHC-coordinated ruthenium alkylidene complexes, see: (a) Prühs, S.; Lehmann, C. W.; Fürstner, A. *Organometallics* **2004**, *23*, 280. For aryloxy-NHC-coordinated ruthenium alkylidene complexes, see: (b) Occhipinti, G.; Bjørsvik, H.-R.; Törnroos, K. W.; Fürstner, A.; Jensen, V. R. *Organometallics* **2007**, *26*, 4383. For an *in situ* generated alkylidene complex active in ROMP of norbonene bearing a sterically crowded aryloxy-NHC, see: (c) Kong, Y.; Xu, S.; Song, H.; Wang, B. *Organometallics* **2012**, *31*, 5527. For arene-NHC-coordinated allenylidene complexes, see: (d) Çetinkaya, B.; Demir, S.; Özdemir, I.; Toupet, L.; Séméril, D.; Bruneau, C.; Dixneuf, P. H. *New J. Chem.* **2001**, *25*, 519. (e) Çetinkaya, B.; Demir, S.; Özdemir, I.; Toupet, L.; Séméril, D.; Bruneau, C.; Dixneuf, P. H. *Chem. Eur. J.* **2003**, *9*, 2323. (f) Özdemir, I.; Demir, S.; Çetinkaya, B.; Toupet, L.; Castarlenas, R.; Fischmeister, C.; Dixneuf, P. H. *Eur. J. Inorg. Chem.* **2007**, 2862.

(3) (a) Van Veldhuizen, J. J.; Campbell, J. E.; Giudici, R. E.; Hoveyda, A. H. *J. Am. Chem. Soc.* **2005**, *127*, 6877. (b) Gillingham, D. G.; Kataoka, O.; Garber, S. B.; Hoveyda, A. H. *J. Am. Chem. Soc.* **2004**, *126*, 12288. (c) Van Veldhuizen, J. J.; Gillingham, D. G.; Garber, S. B.; Kataoka, O.; Hoveyda, A. H. *J. Am. Chem. Soc.* **2003**, *125*, 12502. (d) Van Veldhuizen, J. J.; Garber, S. B.; Kingsbury, J. S.; Hoveyda, A. H. *J. Am. Chem. Soc.* **2002**, *124*, 4954. (e) Gillingham, D. G.; Hoveyda, A. H. *Angew. Chem., Int. Ed.* **2007**, *46*, 3860.

(4) (a) Keitz, B. K.; Endo, K.; Patel, P. R.; Herbert, M. B.; Grubbs, R. H. *J. Am. Chem. Soc.* **2012**, *134*, 693. (b) Endo, K.; Grubbs, R. H. *J. Am. Chem. Soc.* **2011**, *133*, 8525.

(5) (a) Herrmann, W. A.; Kocher, C.; Gookn, L. J.; Artus, G. R. J. *Chem. Eur. J.* **1996**, *2*, 1627. (b) Yang, C.; Lee, H. M.; Nolan, S. P. *Org. Lett.* **2001**, *3*, 1511. (c) Danopoulos, A. A.; Winston, S.; Gelbrich, T.; Hursthouse, M. B.; Tooze, R. P. *Chem. Commun.* **2002**, 482. (d) Tsoureas, N.; Danopoulos, A. A.; Tulloch, A. A. D.; Light, M. E. *Organometallics* **2003**, *22*, 4750. (e) Focken, T.; Raabe, G.; Bolm, C. *Tetrahedron: Asymmetry* **2004**, *15*, 1693. (f) Lee, H. M.; Chiu, P. L. *Acta Crystallogr.* **2004**, *E60*, 1473. (g) Lee, H. M.; Chiu, P. L.; Zeng, J. Y. *Inorg. Chim. Acta* **2004**, *357*, 4313. (h) Lee, H. M.; Zeng, J. Y.; Hu, C.-H.; Lee, C.-H. *Inorg. Chem.* **2004**, *43*, 6822. (i) Bolm, C.; Focken, T.; Rudolph, J. *Synthesis* **2005**, *3*, 429. (j) Field, L. D.; Messerle, B. A.; Vuong, K. Q.; Turner, P. *Organometallics* **2005**, *24*, 4241. (k) Wang, A.-E.; Xie, J.-H.; Wang, L.-X.; Zhou, Q.-L. *Tetrahedron* **2005**, *61*, 259. (l) Hahn, F. E.; Jahnke, M. C.; Pape, T. *Organometallics* **2006**, *25*, 5927. (m) Barczak, N. T.; Grote, R. E.; Jarvo, E. R. *Organometallics* **2007**, *26*, 4863. (n) Danopoulos, A. A.; Tsoureas, N.; Macgregor, S. A.; Smith, C. *Organometallics* **2007**, *26*, 253. (o) Lee, C. C.; Ke, W. C.; Chan, K. T.; Lai, C. L.; Hu, C. H.; Lee, H. M. *Chem.—Eur. J.* **2007**, *13*, 582. (p) Miranda-Soton, V.; Grotjahn, D. B.; DiPasquale, A. G.; Rheingold, A. L. *J. Am. Chem. Soc.* **2008**, *130*, 13200. (q) Shaghafi, M. B.; Kohn, B. L.; Jarvo, E. R. *Org. Lett.* **2008**, *10*, 4743. (r) Song, G.; Wang, X.; Li, Y.; Li, X. *Organometallics* **2008**, *27*, 1187. (s) Benhamou, L.; Wolf, J.; César, V.; Labande, A. S.; Poli, R.; Lugan, N. L.; Lavigne, G. *Organometallics* **2009**, *28*, 6981. (t) Hahn, F. E.; Naziruddin, R. A.; Hepp, A.; Pape, T. *Organometallics* **2010**, *29*, 5283. (u) Cabeza, J. A.; Damonte, M.; García-Álvarez, P.; Kennedy, A. R.; Pérez-Carreño, E. *Organometallics* **2011**, *30*, 826. (v) Cabeza, J. A.; Damonte, M.; García-Álvarez, P.; Hérnández-Cruz, M. G.; Kennedy, A. R. *Organometallics* **2012**, *31*, 327.

(6) (a) Ho, C.-C.; Chatterjee, S.; Wu, T.-L.; Chan, K.-T.; Chang, Y.-W.; Hsiao, T.-H.; Lee, H. M. *Organometallics* **2009**, *28*, 2837.

(b) Naziruddin, A. R.; Hepp, A.; Pape, T.; Hahn, F. E. *Organometallics* **2011**, *30*, 5859.
(7) (a) Karsch, H. H. *Z. Naturforsch., B: Anorg. Chem. Org. Chem.* **1983**, *38*, 1027. (b) Hofmann, P.; Heiss, H. Ger. Pat. DE 41 34 772, 1991 (BASF AG). (c) Feldman, J.; Hauptmann, E.; McCord, E. F.; Brookhart, M. S. World Pat. WO 98/47934, 1998 (DuPont). (d) Eisenträger, F.; Göthlich, A.; Gruber, I.; Heiß, H.; Kiener, C. A.; Krüger, C.; Notheis, J. U.; Rominger, F.; Scherhag, G.; Schultz, M.; Straub, B. F.; Volland, M. A. O.; Hofmann, P. *New J. Chem.* **2003**, *27*, 540.
(8) Hansen, S. M.; Volland, M. A. O.; Rominger, F.; Eisenträger, F.; Hofmann, P. *Angew. Chem., Int. Ed.* **1999**, *38*, 1273.
(9) Pörschke, K.-R.; Pluta, C.; Proft, B.; Lutz, F.; Krüger, C. *Z. Naturforsch.* **1993**, *48b*, 608.
(10) (a) Volland, M. A. O.; Hansen, S. M.; Rominger, F.; Hofmann, P. *Organometallics* **2004**, *23*, 800. (b) Volland, M. A. O.; Straub, B. F.; Gruber, I.; Rominger, F.; Hofmann, P. *J. Organomet. Chem.* **2001**, *617*−*618*, 288. (c) Volland, M. A. O.; Adlhart, C.; Kiener, C. A.; Chen, P.; Hofmann, P. *Chem. Eur. J.* **2001**, *7*, 4621.
(11) NHCP **5a** has been mentioned earlier by us: Gross, J. H; Nieth, N.; Linden, H. B.; Blumbach, U.; Richter, F. J.; Tauchert, M. E.; Tompers, R.; Hofmann, P. *Anal. Bioanal. Chem.* **2006**, *386*, 52 In this paper a Ni-chelate complex of **5a** was reported without any details given, as this compound was just utilized as one sample among others in order to introduce the LIFDI MS technique for typical air- and water-sensitive organometallic compounds..
(12) Hahn, F. E.; Jahnke, M. C. *Angew. Chem.* **2008**, *120*, 3166; *Angew. Chem., Int. Ed.* **2008**, *47*, 3122.
(13) (a) Langhans, K. P.; Stelzer, O.; Weferling, N. *Chem. Ber* **1990**, *123*, 995. (b) Lindner, E.; Neese, P.; Hiller, W.; Fawzi, R. *Organometallics* **1986**, *5*, 2030. (c) Karsch, H. H. *Chem. Ber.* **1982**, *115*, 823. (d) Grim, S. O.; Barth, R. C. *J. Organomet. Chem.* **1975**, *94*, 327. (e) Hellmann, H.; Bader, J.; Birkner, H.; Schumacher, O. *Liebigs Ann. Chem.* **1962**, *659*, 49.
(14) Yarkevich, A. N.; Tkachenko, S. E.; Tsvetkov, E. N. *Zh. Obsch. Khim.* **1990**, *60*, 1511; *Russ. J. Gen. Chem.* **1990**, 1351.
(15) Arduengo, A. J., III; Bock, H.; Chen, H.; Denk, M.; Dixon, D. A.; Green, J. C.; Herrmann, W. A.; Jones, N. L.; Wagner, M.; West, R. *J. Am. Chem. Soc.* **1994**, *116*, 6641.
(16) Koopmans, T. *Physica (The Hague)* **1934**, *1*, 104.
(17) (a) Frisch, M. J.; Trucks, G. W.; Schlegel, H. B.; Scuseria, G. E.; Robb, M. A.; Cheeseman, J. R.; Montgomery, J. A., II; Vreven, T.; Kudin, K. N.; Burant, J. C.; Millam, J. M.; Iyengar, S. S.; Tomasi, J.; Barone, V.; Mennucci, B.; Cossi, M.; Scalmani, G.; Rega, N.; Petersson, G. A.; Nakatsuji, H.; Hada, M.; Ehara, M.; Toyota, K.; Fukuda, R.; Hasegawa, J.; Ishida, M.; Nakajima, T.; Honda, Y.; Kitao, O.; Nakai, H.; Klene, M.; Li, X.; Knox, J. E.; Hratchian, H. P.; Cross, J. B.; Bakken, V.; Adamo, C.; Jaramillo, J.; Gomperts, R.; Stratmann, R. E.; Yazyev, O.; Austin, A. J.; Cammi, R.; Pomelli, C.; Ochterski, J. W.; Ayala, P. Y.; Morokuma, K.; Voth, G. A.; Salvador, P.; Dannenberg, J. J.; Zakrzewski, V. G.; Dapprich, S.; Daniels, A. D.; Strain, M. C.; Farkas, O.; Malick, D. K.; Rabuck, A. D.; Raghavachari, K.; Foresman, J. B.; Ortiz, J. V.; Cui, Q.; Baboul, A. G.; Clifford, S.; Cioslowski, J.; Stefanov, B. B.; Liu, G.; Liashenko, A.; Piskorz, P.; Komaromi, I.; Martin, R. L.; Fox, D. J.; Keith, T.; Al-Laham, M. A.; Peng, C. Y.; Nanayakkara, A.; Challacombe, M.; Gill, P. M. W.; Johnson, B.; Chen, W.; Wong, M. W.; Gonzalez, C.; Pople, J. A. *Gaussian 03*, Revision B.01; Gaussian, Inc.: Wallingford, CT, 2004. (b) Roothaan, C. C. J. *Rev. Mod. Phys.* **1951**, *23*, 69. (c) Petersson, G. A.; Bennett, A.; Tensfeldt, T. G.; Al-Laham, M. A.; Shirley, W. A.; Mantzaris, J. *J. Chem. Phys.* **1988**, *89*, 2193. (d) Petersson, G. A.; Al-Laham, M. A. *J. Chem. Phys.* **1991**, *94*, 6081.
(18) Hansen, S. M.; Rominger, F.; Metz, M.; Hofmann, P. *Chem. Eur. J.* **1999**, *5*, 557.
(19) Brookhart, M.; Green, M. L. H.; Parkin, G. *Proc. Natl. Acad. Sci. U. S. A.* **2007**, *104*, 6908.
(20) (a) Montag, M.; Efremenko, I.; Cohen, R.; Leitus, G.; Shimon, L. J. W.; Diskin-Posner, Y.; Ben-David, Y.; Martin, J. M. L.; Milstein, D. *Chem. Eur. J.* **2008**, *14*, 8183. (b) Albinati, A.; Anklin, C. G.; Ganazzoli, F.; Rüegg, H.; Pregosin, P. S. *Inorg. Chem.* **1987**, *26*, 503. (c) Albinati, A.; Arz, C.; Pregosin, P. S. *Inorg. Chem.* **1987**, *26*, 508. (d) Sundquist, W. I.; Bancroft, D. P.; Lippard, S. J. *J. Am. Chem. Soc.* **1990**, *112*, 1590. (e) Bortolin, M.; Bucher, U.; Reugger, H.; Venanzi, L. M.; Albinati, A.; Lianza, F. *Organometallics* **1992**, *11*, 2514. (f) Cano, M.; Heras, J. V.; Maeso, M.; Alvaro, M.; Fernndez, R.; Pinilla, E.; Campo, J. A.; Monge, A. *J. Organomet. Chem.* **1997**, *534*, 159. (g) Zhang, Y.; Lewis, J. C.; Bergman, R. G.; Ellman, J. A.; Oldfield, E. *Organometallics* **2006**, *25*, 3515.
(21) (a) Becke, A. D. *Phys. Rev. A* **1988**, *38*, 3098. (b) Perdew, J. P. *Phys. Rev. B* **1986**, *33*, 8822. (c) Perdew, J. P. *Phys. Rev. B* **1986**, *34*, 7406.
(22) Klamt, A.; Schüürmann, G. *J. Chem. Soc., Perkin Trans. 2* **1993**, *5*, 799.
(23) (a) Fogg, D. E.; James, B. R. *Inorg. Chem.* **1997**, *36*, 1961. (b) Joshi, A. M.; Thorburn, I. S.; Rettig, S. J.; James, B. R. *Inorg. Chim. Acta* **1992**, *198*−*200*, 283.
(24) Schwab, P.; Grubbs, R. H.; Ziller, J. W. *J. Am. Chem. Soc.* **1996**, *118*, 100.
(25) Elemental analyses for the Ru carbenes **7b**−**f** in all cases are somewhat outside the range associated with full analytical purity. NMR spectra showed relatively clean compounds (viz. SI), correct HR MS characterizations are available, and single-crystal X-ray structure determinations could be performed.
(26) Mothes, E.; Sentets, S.; Luquin, M. A.; Mathieu, R.; Lugan, N.; Lavigne, G. *Organometallics* **2008**, *27*, 1193.
(27) (a) Nguyen, S. D.; Johnson, L. K.; Grubbs, R. H. *J. Am. Chem. Soc.* **1992**, *114*, 3974. (b) Schwab, P.; Grubbs, R. H.; Ziller, J. W. *J. Am. Chem. Soc.* **1996**, *118*, 100. (c) Schwab, P.; France, M. B.; Ziller, J. W.; Grubbs, R. H. *Angew. Chem.* **1995**, *107*, 2179; *Angew. Chem., Int. Ed. Engl.* **1995**, *34*, 2039. (d) Wilhelm, T. E.; Belderrain, T. R.; Brown, S. N.; Grubbs, R. H. *Organometallics* **1997**, *16*, 3867. (e) Olivan, M.; Caulton, K. G. *Chem. Commun.* **1997**, 1733. (f) Belderrain, T. R.; Grubbs, R. H. *Organometallics* **1997**, *16*, 4001. (g) Grünwald, C.; Gevert, O.; Wolf, J.; Gonzales-Herrero, P.; Werner, H. *Organometallics* **1996**, *15*, 1960. (h) Wolf, J.; Stüer, W.; Grünwald, C.; Werner, H.; Schwab, P.; Schulz, M. *Angew. Chem.* **1998**, *110*, 1165. (i) Chang, S.; Jones, L.; Wang, C. M.; Henling, L. M.; Grubbs, R. H. *Organometallics* **1998**, *17*, 3460. (j) Herrmann, W. A.; Weskamp, T.; Kohl, F. J.; Schattenmann, W. C.; Nuyken, O.; Frenzel, U. XVIIIth ICOMC, Poster B105, Munich 1998. (k) Herrmann, W. A.; Weskamp, T.; Schattenmann, W. C. XVIIIth ICOMC, Poster B106, Munich 1998. (l) Katayama, H.; Yoshida, T.; Ozawa, F. *J. Organomet. Chem.* **1998**, *562*, 203. (m) Fürstner, A.; Piquet, M.; Bruneau, C.; Dixneuf, P. H. *Chem. Commun.* **1998**, 1315.
(28) Volland, M. A. O.; Rominger, F.; Eisenträger, F.; Hofmann, P. *J. Organomet. Chem.* **2002**, *641*, 220.
(29) Wang, H. M. J.; Lin, I. J. B. *Organometallics* **1998**, *17*, 972.
(30) Helmchen, G.; Bappert, E. *Synlett* **2004**, 1789.
(31) Fürstner, A.; Guth, O.; Düffels, A.; Seidel, G.; Liebl, M.; Gabor, B.; Mynott, R. *Chem. Eur. J.* **2001**, *7*, 4811.
(32) (a) Arduengo, A. J., III; Gentry, F. P., Jr.; Taverkere, P. K.; Simmons, H. E., III US Patent No. 6,177,575 B1 Du Pont, Jan 23, 2001. (b) Gridnev, A. A.; Mihaltseva, I. M. *Synth. Commun.* **1994**, *24*, 1547.
(33) Strassner, T.; Ahrends, S. Patent No. WO 2009/095012 A1, Aug 6, 2009.
(34) Creary, X. *Org. Synth.* **1986**, *64*, 207.